



Recent advances in chemically defined and tunable hydrogel platforms for organoid culture

Tarun Agarwal¹ · Nehar Celikkin² · Marco Costantini² · Tapas K. Maiti¹ · Pooyan Makvandi³

Received: 2 October 2020 / Accepted: 6 January 2021 / Published online: 7 February 2021
 © Zhejiang University Press 2021

Abstract

Recent developments in organoid culture technologies have made it possible to closely recapitulate intrinsic characteristics of different tissues under in vitro conditions. These organoids act as a translational bridge between the traditional 2D/3D cultures and the in vivo models for studying the tissue development processes, disease modeling, and drug screening. Matrigel and tissue-specific extracellular matrix have been shown to support organoid development, efficiently; however, their chemically undefined nature, non-tunable properties, and associated batch-to-batch variations often limit reproducibility of the assembly process. In this regard, chemically defined platforms offer wider opportunities to optimize and recreate tissue-specific micro-environment. The present review delineates the current research trends in this sphere, focusing on material perspective and the target tissues (e.g., neural, liver, pancreatic, renal, and intestinal). The review winds up with a discussion on the current limitations and future perspective to provide a basis for future research.

Keywords Organoid · 3D culture · Biomaterials · Chemically defined hydrogels · Cell-instructive microenvironment

Abbreviations

2D	Two dimensional	MSC	Mesenchymal stem cells
3D	Three dimensional	FN	Fibronectin
SD	Standard deviation	DV	Dorsal–ventral
ECM	Extracellular matrix	iPSCs	Induced pluripotent stem cells
EHS	Engelbreth–Holm–Swarm	ALB	Albumin
LMN	Laminin	MDR1	Multidrug resistance protein 1
COLIV	Collagen IV	CNF	Cellulose nanofibril
HA	Hyaluronic acid	ALAT	Alanine aminotransferase
PEG	Polyethylene glycol	ASAT	Aspartate transaminase
PIC	Polyisocyanopeptide	PEGDE	Poly(ethylene glycol) diglycidyl ether
MMPs	Matrix metalloproteinases	LGR5	Leucine-rich repeat-containing G-protein-coupled receptor 5
GLDH	Glutamate dehydrogenase	BME2	Basement Membrane Extract Type 2
ESCs	Embryonic stem cells	dPMP	Degradable PEG-MMP-PEG
HSPCs	Hematopoietic stem and progenitor cells	ndPH	Non-degradable PEG–heparin
BMSCs	Bone marrow stromal cells	dPMH	Degradable PEG-MMP-Heparin
PEGDA	Poly(ethylene glycol) diacrylate	LEC	LMN–entactin complex
		HNF4 α	Hepatocyte nuclear factor 4 α
		E-cad	E-cadherin
		KRT19	Cytokeratin 19
		NHE3	Sodium–hydrogen exchanger 3
		Muc2	Mucin 2
		Lyz	Lysozyme

✉ Tapas K. Maiti
 tkmaiti@hijli.iitkgp.ernet.in; maititapask@gmail.com

¹ Department of Biotechnology, Indian Institute of Technology Kharagpur, Kharagpur, West Bengal 721302, India

² Institute of Physical Chemistry – Polish Academy of Sciences, Warsaw, Poland

³ Centre for Micro-BioRobotics, Istituto Italiano di Tecnologia, Viale Rinaldo Piaggio 34, 56025 Pontedera, Pisa, Italy

Introduction

Consistent efforts toward developing biomimetic complex tissue structures have unfolded strategies for organoids' growth and maintenance under *in vitro* conditions [1–3]. Organoids could be generated from stem cells, progenitor cells, or even tissue fragments, which undergo self-organization to form tissue-like structures, exhibiting key architectural and functional features along with multicellular complexity, similar to native ones [3, 4]. To date, organoids equivalents of different organs including (but not limited to) gastrointestinal [5–7], pancreatic [8, 9], hepatic [10, 11], renal [12, 13], endometrial [14, 15], cardiac [16, 17], retinal [18, 19], lungs [20, 21], immune [22, 23], neural [24, 25], and skin [26, 27] have been generated. These organoids are believed to have endless translational applicability in R&D, healthcare, diagnostics, and pharmaceutical sectors as they address many limitations of current *in vitro* and *in vivo* models [3, 4]. Besides, organoids' potential implementation as a cell-based therapy for tissue repair and regeneration cannot be overlooked [28].

The traditional method of generating organoids relies on the use of complex animal-derived extracellular matrix (ECM) hydrogels, primarily Matrigel, with a recent inclination toward tissue-specific ECM [28–35]. Matrigel is a solubilized basement membrane preparation derived from the Engelbreth–Holm–Swarm (EHS) mouse sarcoma. It majorly consists of laminin (LMN), collagen IV (COLIV), entactin, and heparin sulfate proteoglycan, along with several growth factors [28, 29]. On the other hand, tissue-specific ECM is derived from tissues/organs using decellularization procedures; the obtained ECM is further solubilized to form a pre-gel solution [31, 36, 37]. The stem cells or tissue fragments encapsulated in these hydrogels undergo morphogenesis to form tissue organoids via interaction with various biochemical/biophysical cues offered by the hydrogel [28–30]. Although these gold standard animal-derived materials have been shown to sustain the growth and long-term culture of almost all the known organoids, to date, they have their limitations [28, 29]. Compositionally, both these matrices are still ill-defined, contain xenogenic constituents and growth factors, and suffer batch-to-batch variability, thereby introducing variability in organoid assembly and developmental processes [28, 29]. Moreover, the lack of control over different tunable properties, including biochemical, biomechanical, and biodegradation, further impedes their advancements [28–30]. Cancerous origin of Matrigel also limits its translational aspects [28].

In this regard, organoid culture technology has evidenced increasing efforts to explore chemically defined alternatives [28–30]. Such platforms offer to tune intricate

components of the tissue microenvironment and guide the formation, maintenance, and differentiation of organoids in a controlled and reproducible manner [28–30, 35]. The current review highlights developments in organoid technology employing chemically defined hydrogel platforms.

Chemically defined hydrogels: cell-instructive behavior

The organoid formation is a dynamic process; hence, the matrix that encapsulates the organoid should also be dynamic. Cell–matrix interaction is one of the dominant determinants in translating single cells into organized and structured 3D forms. During organoid formation, the matrix characteristics significantly impact cell viability, proliferation, cell–cell crosstalk, cytoskeletal changes, and homeostasis, controlled in a spatiotemporal manner (Fig. 1) [38].

Early organoid studies have used solubilized decellularized ECM, thanks to its complex tissue-specific composition, favorable mechanical properties, and biocompatibility. Nevertheless, batch-to-batch differences in ECM composition and mechanical properties, unfortunately, resulted in a lack of reproducibility of these results [35]. Therefore, various natural and synthetic biomaterials were adapted into organoid research to improve the standardization of the process. The presence of adhesion motifs, mechanical properties, biodegradability, cross-linking conditions, and the biocompatibility of these natural and synthetic biomaterials are remarked as the distinctive selection criteria. They play a substantial role in creating a dynamic microenvironment for the organoid cultures. For instance, while the presence or density of the adhesion motifs on the polymeric backbone intermediates and affects cytoskeletal dynamics and morphogenesis, the bulk/localized matrix mechanical properties control mechanotransduction-associated cell signaling cascades [39]. Even the variability in the motif type or density could also modulate cellular phenotype. RGDS motif, but not RGES, better supported the human hepatocytes' functional characteristics [40]. In another study, the presence of RGD motifs at high density was shown to inhibit osteogenesis while promoting adipogenic differentiation of mesenchymal stem cells (MSCs) [41].

Chemically defined hydrogels: material perspective

Up to date, the proposed chemically defined natural and synthetic biomaterials cannot yet recapitulate the natural ECM composition complexity, structure, and bioactivity. However, the precise and consistent production of these materials ensures high reproducibility and effective customization.

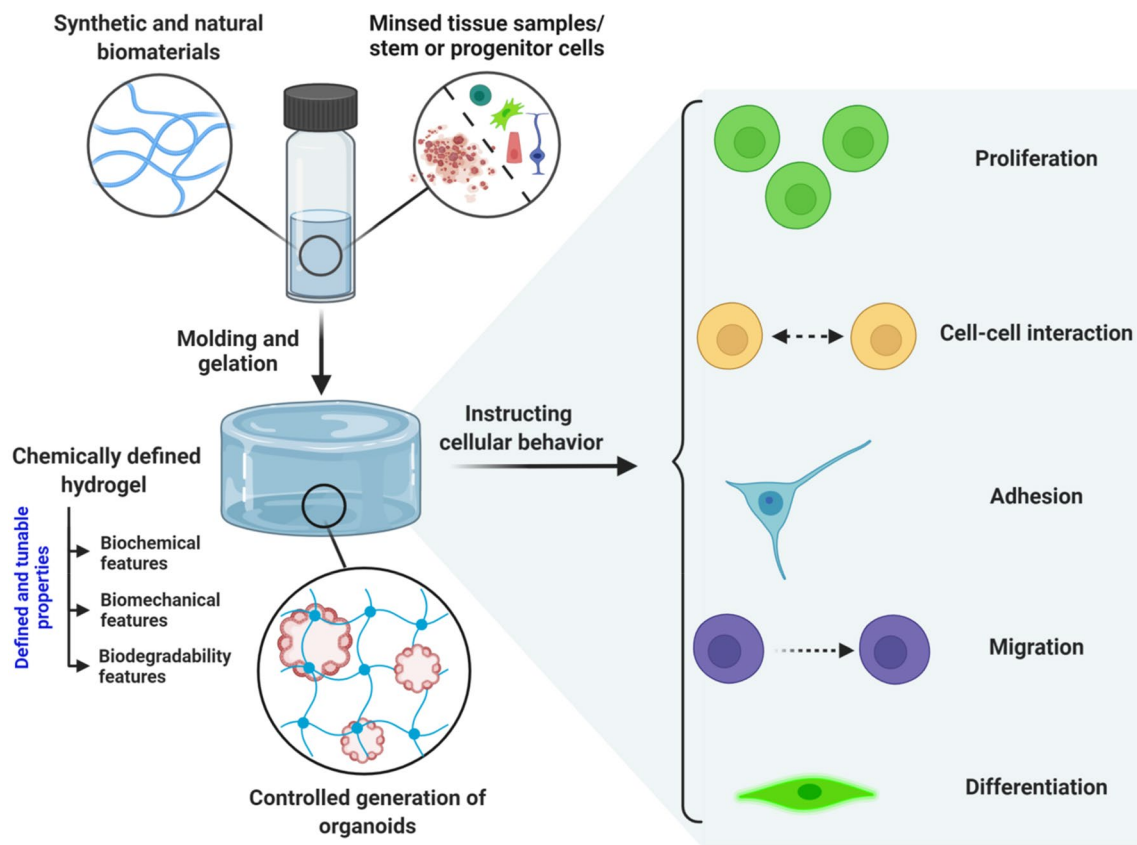


Fig. 1 Schematic of defined hydrogels with tunable physicochemical properties to instruct cellular behaviors in building 3D organoid models

Aiming to reduce the complexity and increase the experiment reproducibility, natural single biopolymer components such as collagen type I, gelatin, hyaluronic acid (HA), alginate, fibrin or mixtures thereof have been investigated [35]. However, small differences in matrix composition or biopolymer properties are still present that could negatively affect the results' reproducibility. Therefore, matrices entirely based on synthetic polymers have also been considered [29]. Polyethylene glycol (PEG) and polyisocyanopeptide (PIC) are the two pioneer synthetic polymers used closely in organoid research. Table 1 presents a comparative evaluation of natural and synthetic materials in different aspects.

Natural biomaterials and their derivatives

Single biopolymer components based on natural protein, glycosaminoglycans, and polysaccharide are used in organoid research [35]. Among protein-based biopolymers, collagen type I, gelatin, and fibrin are the most popular ones. Collagen is the most abundant ECM protein in the vertebrates, while gelatin is a collagen derivative [42, 43]. The primary structure of collagen is a triple-stranded helix that is responsible for collagen's thermo-responsive characteristic. Depending on the chemical composition, pH,

and temperature, collagen can self-assemble into strong, long cross-linked fibrils. Thanks to its significant mechanical properties, collagen type I is resistant to tensile forces, thus typically used in connective tissue organoids [44–47]. Despite collagen's desirable biochemical characteristics, its limited solubility in cell-friendly conditions hinders its processability.

Unlike collagen, gelatin's high solubility in the water at physiological temperature allows its easy processability while maintaining a proper cell environment. As gelatin is water-soluble at physiological temperatures, permanent cross-linking of gelatin matrices is ensured through chemical or enzymatic polymerization using Genipin or transglutaminase [48, 49]. Additionally, photoinitiated radical polymerization is also prevalently used for cross-linking of gelatin matrices; nevertheless, for such applications, gelatin should be functionalized with acrylic/methacrylic moieties [50]. Fibrinogen is another abundant protein in vertebrates, although to a lesser extent compared to collagen. Fibrinogen can naturally self-assemble into fibrin in the presence of thrombin to form a gel [51]. Like gelatin and collagen, fibrin also possesses different cell adhesion motifs, including RGD, allowing it to support cell viability, proliferation, hemostasis, differentiation, and function without any further

Table 1 Summary of the distinctive hallmarks of biomaterials suited for developing organoids

Biomaterials	Distinctive hallmarks	Cross-linking mechanism	Source	Cost	References
<i>Natural hydrogels</i>					
Collagen	Intermolecular cross-links among the triple-helical structures pH- and temperature-dependent self-assembling fibril-forming properties Amino acid repeating sequence [Gly-X-Y] _n , X positions by proline and Y positions by hydroxyproline	Physical gelation: Thermal self-assembly Chemical gelation: Glutaraldehyde, EDC/NHS, photopolymerization (methacrylate, thiol derivatives)	Bovine skin and tendons, porcine skin, rat tail, sponges, fish, shark, and jellyfish	\$\$\$	[77, 78]
Gelatin	Derived through hydrolytic processes of collagen Molecular weight can be controlled through the hydrolytic processing parameters such as pH, temperature, and time Amino acid repeating sequence [Gly-X-Y] _n , X positions by proline and Y positions by hydroxyproline	Physical gelation: Thermal self-assembly Chemical gelation: Glutaraldehyde, EDC/NHS, photopolymerization (methacrylate, thiol derivatives) Enzymatic gelation: Transglutaminase	Bovine skin and tendons, porcine skin, rat tail, sponges, fish, shark, and jellyfish	\$	[79, 80]
Fibrinogen	A complex triglobular, elongated protein Capable of conveying matrix proteins such as fibronectin and growth factors Possess both strong and weak binding sites for calcium ions Thermal and enzymatic clotting	Enzymatic gelation: Thrombin, Factor XIII Chemical gelation: Glutaraldehyde, EDC/NHS	Human plasma, bovine plasma, rat plasma	\$\$\$	[81]
Heparin	Linear polysaccharide Made up of repeating disaccharides, primarily uronic acid and glucosamine with varying degrees of sulfation and <i>N</i> -acetylation High affinity for growth factors	Physical gelation: Electrostatic interaction Chemical gelation: Photopolymerization (thiol, maleimide derivatives)	Porcine intestinal mucosa, intestinal tissue of Turkey, bovine lung	\$	[57, 82]
Hyaluronic acid	Non-sulfated anionic polysaccharide from glycosamine glycan family Composed of repeating units of disaccharides <i>D</i> -glucuronic acid and <i>N</i> -acetyl- <i>D</i> -glucosamine Specific binding site for CD44	Chemical gelation: Glutaraldehyde, EDC/NHS, Photopolymerization (methacrylate, thiol derivatives)	Bacterial <i>Streptococcus equi</i> , bacterial <i>Streptococcus pyrogenes</i> , bovine vitreous humor, rooster comb	\$\$\$	[83, 84]
Alginate	A natural anionic polysaccharide It is composed of repeating units of β - <i>D</i> -mannuronic acid (M) and α - <i>L</i> -guluronic acid (G) residues Low protein adsorption	Physical gelation: Ionic cross-linking, electrostatic interaction Chemical gelation: Glutaraldehyde, EDC/NHS, photopolymerization (methacrylate, thiol derivatives)	Brown algae, including <i>Laminaria hyperborea</i> , by treatment with aqueous alkali solutions	\$	[85–87]
Chitosan	A linear polysaccharide consisting of <i>N</i> -acetylglucosamine and <i>N</i> -glucosamine repeating units Cationic molecules possessing abundantly functional amine and hydroxyl groups on the molecular chain An excellent protein binding Antimicrobial characteristics	Physical gelation: Ionic cross-linking, Electrostatic interaction Chemical gelation: Glutaraldehyde, EDC/NHS, photopolymerization (methacrylate, thiol derivatives)	Exoskeleton of crustaceans	\$	[88, 89]

Table 1 (continued)

Biomaterials	Distinctive hallmarks	Cross-linking mechanism	Source	Cost	References
<i>Synthetic hydrogels</i>					
PEG	Non-ionic synthetic hydrophilic polymer Available in different molecular weights (300 Da–40 kDa) Efficient cell binding to the once functionalized with conjunction of cell adhesion peptides	Chemical gelation: Photopolymerization, click chemistry, radical polymerization	Synthetic (N/A)	\$\$	[90–92]
PIC	Exhibit reversible thermo-responsive self-assembly Strain-stiffening property Efficient cell binding to the once functionalized with conjunction of cell adhesion peptides	Physical gelation: Thermal self-assembly Chemical gelation: Click chemistry	Synthetic (N/A)	-	[69, 75, 76]

\$: 1\$ < price per gram polymer < 10\$, \$\$: 10\$ < price per gram polymer < 100\$, \$\$\$: 100\$ < price per gram polymer

functionalization. Hence, fibrin can enable long-term expansion of organoids [52, 53].

Besides protein-based biopolymers, glycosaminoglycans also hold great potential for designing dynamic organoid microenvironment. For example, HA matrices can activate cascade signals which affect cell attachment, migration, proliferation, and morphogenesis thanks to their capacity of interaction with several cell transmembrane receptors such as CD44, CD54, and CD168 [54]. However, the resilience of HA hydrogels and their ability to resist degradation by hyaluronidases, reactive oxygen and nitrogen species, highly hinder their applicability. In order to improve HA degradation, protease-sensitive motifs such as that of matrix metalloproteinases (MMPs) have been exploited for preparing HA-based platforms [55, 56]. Heparin is another natural glycosaminoglycan that has witnessed broad applicability for tissue engineering, mainly due to its anticoagulant and antithrombotic properties [57]. Owing to its negative charge, it also has a high affinity for various growth factors [57, 58]. Moreover, sulfonic acid, hydroxyl, and carboxyl groups on the heparin backbone enable functionalization with light-sensitive moieties and conjugation with synthetic and natural polymers to create multifunctional 3D matrices for organoid cultures [59, 60].

Additionally, polysaccharides have also been abundantly employed in organoid research, alginate being the most favorable one due to its biocompatibility and ease of manipulation [61, 62]. The cross-linking of alginate could occur in the presence of di-/trivalent cations under physiological conditions, averting a need for its further modification [63]. However, due to the lack of cell adhesive moiety, alginate often requires either functionalization with cell-binding cues or mixed with more instructive biopolymers to support organoid formation [45, 64]. Chitosan is another natural polysaccharide, derived from the partial deacetylation of chitin; its chemical structure constitutes D-glucosamine and N-acetyl-D-glucosamine [65, 66]. Unlike alginate, chitosan is protonated in acidic aqueous solutions and acts as a polycationic polymer. Thanks to its polycationic behavior, chitosan can form polyionic complexes with different anionic polymers (such as HA, gelatin, chondroitin sulfate) and thus could be utilized for organoid culture [67]. Besides, the amine groups on its backbone provide an opportunity to conjugate biologically active molecules (fibronectin (FN), LMN, and other peptides/proteins) to support cell growth and differentiation [68].

Synthetic biomaterials and their derivatives

Biocompatible synthetic polymers have also been studied extensively in the last decades, with the most common materials being polyvinyl alcohols, PEG, PIC, and polyacrylamide and their derivatives. PEG and PIC derivatives

come forward in organoid research as they closely mimic the fibrous and porous architecture and mechanical properties of structural ECM proteins (Fig. 2) [69, 70]. PEG-based hydrogels are prevalently used in this research area as they are commercially available in a wide range of structures (for example, linear or multi-arm star versions) and molecular weights, enabling different matrix designs, mechanical and rheological properties [71, 72]. Moreover, they can easily be functionalized, using thiol-ene or azide-alkyne chemical strategies, to incorporate different biological ligands, signaling molecules, and cross-linking/degradation sites, allowing the precise tuning of physical and biochemical niche properties [73, 74]. These reactions are rapid and quantitative in yield, making them attractive tools for the fabrication of functionalized PEG hydrogels.

On the other hand, PICs are a relatively newer class of synthetic hydrogels employed for organoid research due to their thermo-responsive nature [69]. Rapid gelation of PIC solutions can thermally be induced by heating them beyond the gelation temperature ($T_{gel} \approx 18\text{ }^{\circ}\text{C}$). Moreover, PIC gelation is fully reversible, particularly advantageous

for cell and organoid extraction [69, 75]. Regarding the mechanical properties, PIC hydrogels can be formed at low polymer concentrations (0.1–1 wt%), and they display low shear modulus $G' = 0.1\text{--}4\text{ kPa}$ that overlaps with the stiffness of various soft tissues [69]. Despite these attractive properties, PIC hydrogels lack cell-binding sites; however, a rapid functionalization with cell adhesion cues such as RGD can be achieved through strain-promoted azide-alkyne cycloaddition reaction [76].

Organoid culture in defined hydrogels

To date, numerous studies have already explored the defined and tunable hydrogels for establishment and growth of organoid cultures, via recreating cell-instructive microenvironment. This section elaborates over such representative studies, segregated based on the different tissue types, including, neural, hepatic, pancreatic, renal, intestinal, and others.

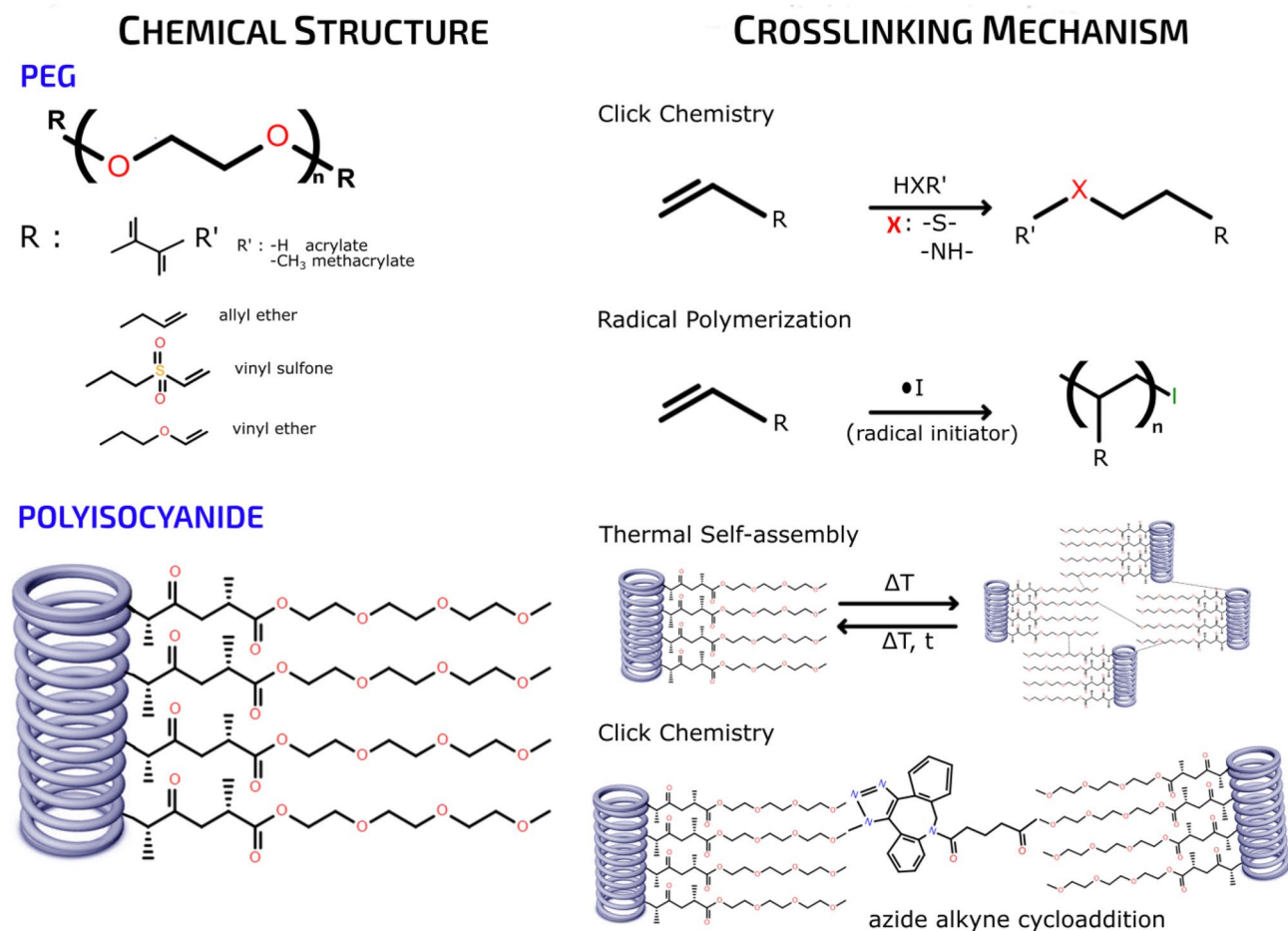


Fig. 2 Chemical structure and cross-linking mechanism of various PEG derivatives and PIC polymer

Neural organoids

The neural development is one of the most complex processes, making it challenging to model and study in the absence of an animal model; however, the recent advancements in cerebral and neural organoid technologies have made it possible, to an extent [93].

In an effort to study early neurogenesis pattern, tunable synthetic hydrogel system was developed and further used for culturing and differentiating mouse embryonic stem cells (ESCs) (Fig. 3) [94]. Hydrogels were formed by 8-arm PEG precursor molecules conjugated with lysine-donor (with/

without MMP-sensitive motif) and glutamine-acceptor factor XIIIa substrate peptides in the presence of thrombin-activated FXIIIa. The hydrogels’ mechanical properties could be tuned via alteration in precursor polymer density, while a change in the ratio of MMP-sensitive and insensitive lysine-donor peptides affected the degradability of gels. The optimal synthetic hydrogel compositions supported the formation of more homogeneous neuroepithelial colonies, a higher proportion of cysts having apicobasal polarity, and neural tubelike patterning along the dorsal–ventral (DV) axis. An in-depth evaluation of tunable characteristics revealed that non-degradable PEG hydrogel with stiffness range between

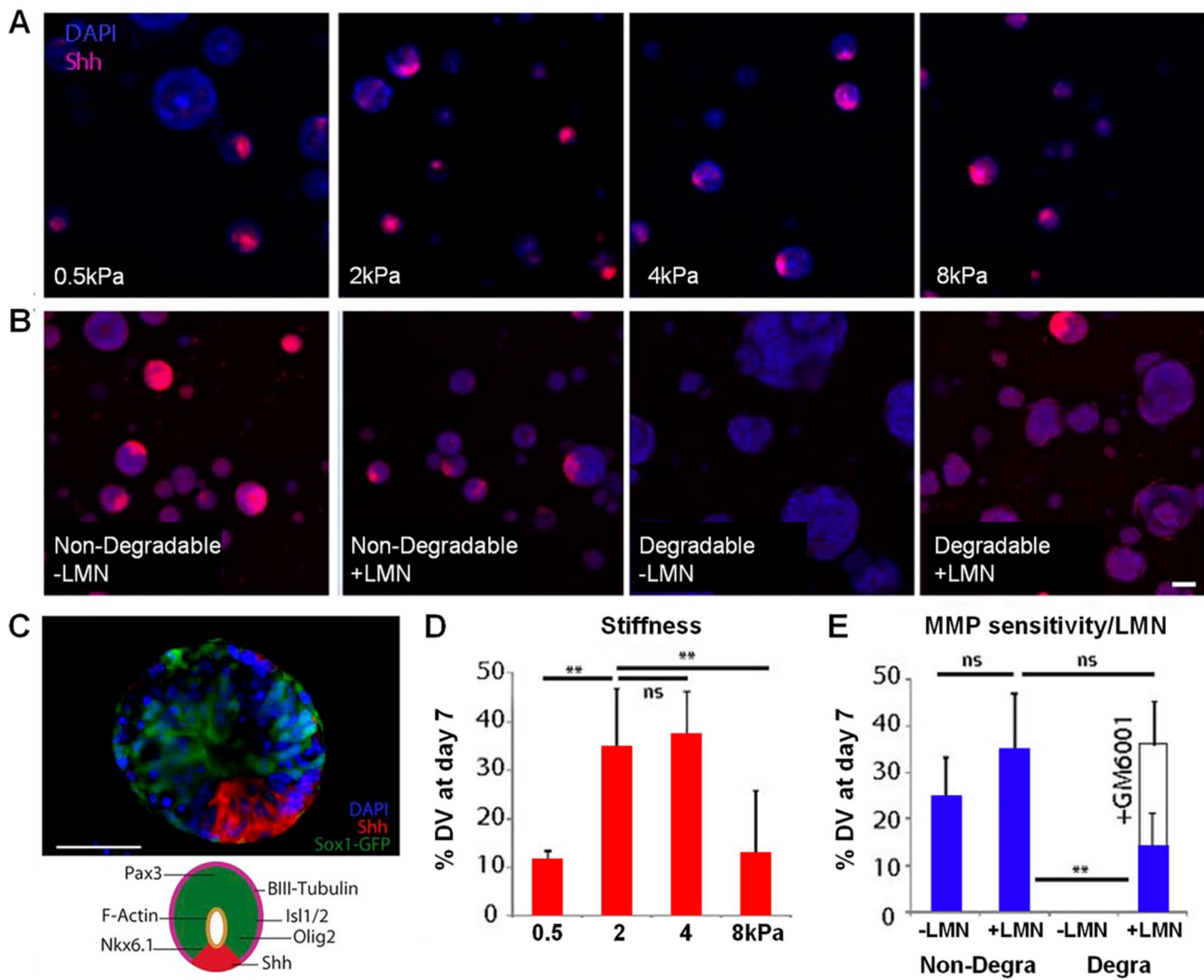


Fig. 3 Representative images of Shh-immunostained neural cysts with DV patterning, cultured in non-degradable PEG matrices with **a** variable stiffness and **b** variable degradability and LMN composition (stiffness ~2 kPa). Nucleus was stained with DAPI. Scale bar: 100 μm. **c** Representative fluorescent micrographs and schematics demonstrating DV patterning with key features of neural tube architecture, Shh+ floor plate, Olig2+ progenitor motor neuron, Isl1/2+ motor neuron, βIII tubulin+ post-mitotic neuron, as well as Nkx6.1+

ventral and Pax3+ dorsal positional identities. Scale bar: 50 μm. Quantitative evaluation of DV patterning efficiency of neural organoids in non-degradable PEG hydrogels with **d** variable stiffness and **e** variable degradability and LMN composition, at day 7 of culture. Error bars: standard error (SE). “***” represents significant difference with *p* value < 0.01. Reproduced with permission from Ref. [94]. Copyright © 2016, Ranga et al.

2 and 4 kPa and supplemented with LMN supported a better progression of neurogenic events. Another two variants of PEG-based synthetic hydrogel with tunable biochemical features, first consisting of PEG-conjugated with collagen-like peptide (PEG-CLP) and the other with collagen-like peptide attached to RGD motif (PEG-CLP-RGD), were reported to support the self-organization of cerebellar cells into functional organoids [95]. PEG-CLP-RGD hydrogels demonstrated a higher neurite outgrowth, though they were not organized as compactly as in PEG-RGD.

Recently, carboxylated HA and protonated chitosan hydrogel (together, termed as Cell-Mate3D matrix) were employed for robust generation of cerebral organoids from human-induced pluripotent stem cells (iPSCs) [67]. In a short culture duration (~10–14 days), in the defined hydrogels, early corticogenesis was observed in the cerebral organoids characterized by the formation of neural rosettes and neural tubelike structures and expression of neural differentiation markers (β -III tubulin, SOX2, nestin). At this stage, the organoid was spherical with a maximum dimension of ~1 mm; which further increased to 2.5–3 mm by 28th day of culture with an increase in their complexity. The cerebral organoids demonstrated an enhanced expression of the forebrain, midbrain, and hindbrain markers; however, the expression levels were greatly influenced by the iPSC line and neural differentiation time. Besides, physiologically relevant glutamate responsiveness and cellular depolarization were also evident in the developed organoids.

Hepatic organoids

The liver is the largest internal organ, consisting of hepatocytes (major population ~70%), biliary epithelial cells, hepatic stellate cells, liver sinusoidal endothelial cells, Kupffer cells, and hepatic stem/progenitor cells, which are organized in unique lobular architecture and carries out over 500 different functions [96, 97]. The emergence of liver organoid technology has provided a newer dimension to the pharmaceutical sector, particularly those linked with the assessment of hepatotoxic drug responses [98–100]. They may also have potential applicability for tissue engineering and disease modeling domain [101].

A recent study demonstrated that synthetic MMP-sensitive, RGD-conjugated PEG hydrogel matrices (PEG-RGD) efficiently supported the formation and differentiation of liver organoids, comparable either to Matrigel or PEG hydrogels conjugated with either COLIV (PEG-COLIV) or LMN-111 (PEG-LAM-1) or fibronectin (PEG-FN) (Fig. 4) [101]. Besides, mechanical aspects also play a critical role in determining the phenotypic characteristics of the liver organoids. To further ascertain its applicability in this domain, PEG-RGD hydrogels of variable stiffness were prepared by altering the polymeric density. The hydrogels mimicking the

physiological liver stiffness ranges (between 1.3 and 1.7 kPa) were optimal for generating liver organoids, while those with lower or higher stiffness limited the process. Interestingly, organoids in PEG-RGD hydrogels (stiffness ~4 kPa) displayed characteristics of fibrotic liver tissue with downregulation of hepatic progenitor cells markers and upregulation of hepatic injury-associated genes. These optimized PEG-RGD hydrogels also offer immense avenues for establishing patient-specific human liver organoids directly from human biopsies, a step toward developing personalized therapies.

Another synthetic hydrogel matrix based on PIC, supplemented with either LMN–entactin complex (PIC-LEC) or recombinant human LMN-111 (PIC-LMN-1), supported the expansion and differentiation of liver organoids; unconjugated PIC (PIC-plain) or RGD-conjugated PIC (PIC-RGD) gels, instead, were insufficient for the same (Fig. 5) [75]. The phenotypic characteristics of organoids were greatly influenced by the molecular weight of PIC (1 kDa or 5 kDa), polymer density (2.5, 1.75, 1 mg/mL), and concentration of LEC/LMN-111 (1, 2, 3 mg/mL). Organoids differentiated in PIC hydrogels exhibited albumin (ALB) secretion, glutamate dehydrogenase (GLDH) production, ammonia elimination, multidrug resistance protein 1 (MDR1) rhodamine 123 transporter activity, and the expression of mature hepatocyte markers, comparable or better than Matrigel. Moreover, the thermo-responsive nature of these PIC hydrogels adds an advantage for organoid subculturing, while maintaining organoid functional characters even after 10 passages.

Alternatively, hydrogels composing a single or composition of multiple biomacromolecules could provide a defined microenvironment for culturing liver organoids. For instance, cellulose nanofibril (CNF) hydrogels supported differentiation of liver organoids with the expression of hepatocyte-specific markers, ALB secretion, glycogen accumulation, GLDH production, alanine aminotransferase (ALAT), and aspartate transaminase (ASAT) activity, comparable or better than those cultured in Matrigel [102]. In another study, composite hydrogel capsules consisting of fibrin core and alginate–chitosan shell were fabricated using droplet microfluidic technique for generating liver organoids from human iPSCs-derived hepatic progenitor cells [53]. Organoids in hydrogel capsules expressed hepatocyte and cholangiocyte markers and showed ALB and urea synthesis. The presence/absence of fibrin hydrogels in the capsule core significantly affected phenotype of the liver organoids.

Pancreatic organoids

The pancreas is a compound gland that exhibits both exocrine (via acinar and ductal cells) and endocrine (alpha, beta, gamma, epsilon, and PP cells) functions, arranged in a specialized manner, forming islets of Langerhans. Pancreatic organoids have great importance for understanding

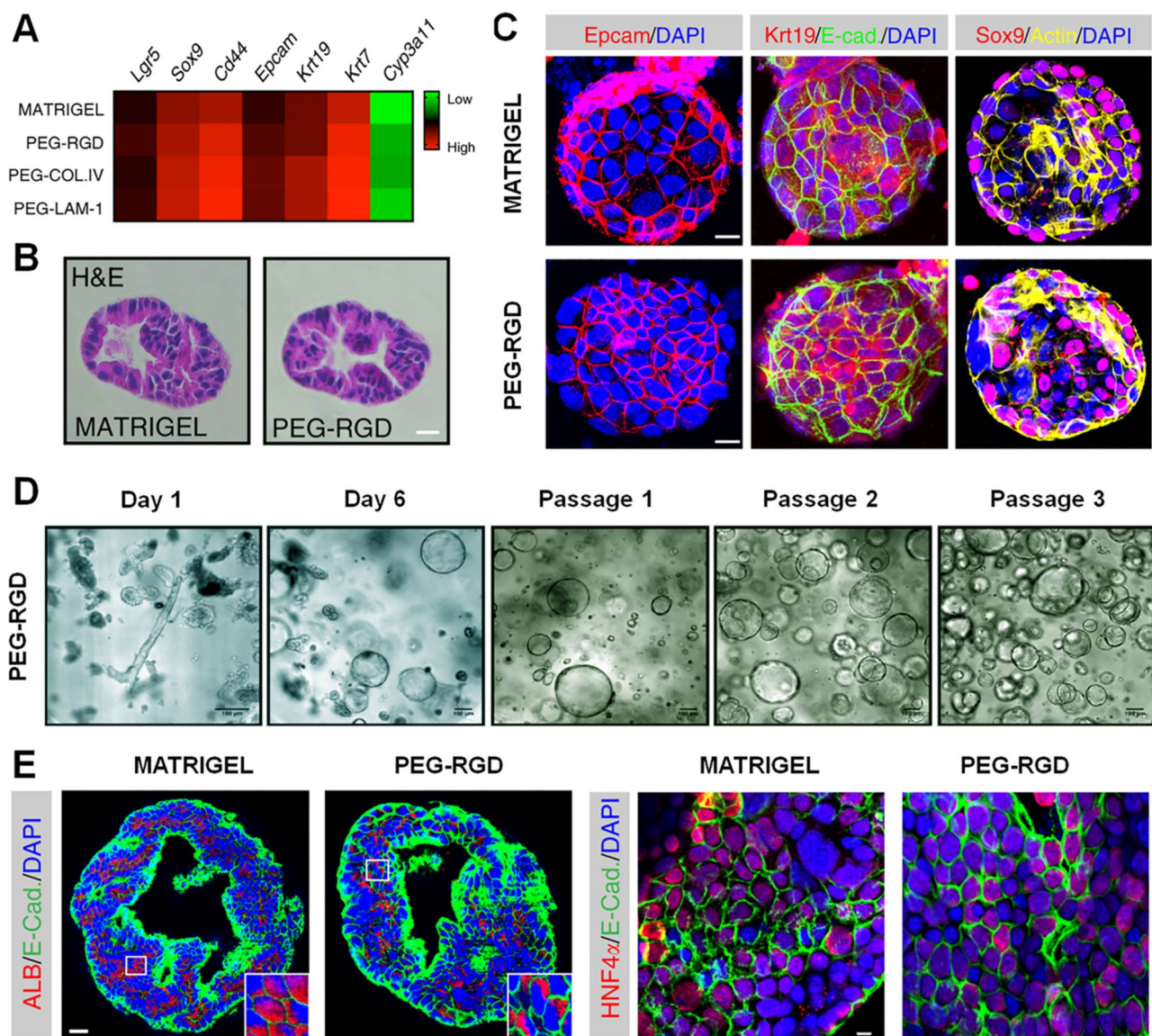


Fig. 4 **a** Heat map representation of gene expression of different markers in liver organoids cultured in Matrigel, PEG-RGD, PEG-COLIV, and PEG-LAM-1. **b** Representative images of H&E stained section of liver organoids cultured in Matrigel and PEG-RGD hydrogels. Scale bar 25 μm . **c** Representative images of immunostained sections of liver organoids in Matrigel and PEG-RGD hydrogels. **d** Bright-field micrographs of liver organoids at different days of seed-

ing and different passages. Scale bar 100 μm . **e** Representative immunofluorescence confocal micrographs of ALB, hepatocyte nuclear factor 4 α (HNF4 α), and E-cadherin (E-cad)-stained liver organoids in Matrigel and PEG-RGD hydrogels. Scale bars: 25 μm (left), 10 μm (right). Reproduced with permission from Ref. [101]. Copyright © 2020, Sorrentino et al.

the disease biology and finding therapeutic interventions, mainly associated with common pancreatic diseases, like diabetes (type 1 or type 2) and cancer [103].

In an attempt to recreate artificial 3D pancreatic niche under in vitro conditions, synthetic MMP-sensitive, soft (shear modulus ~ 250 Pa) PEG-LMN hydrogels were developed [104]. These hydrogels were able to maintain and expand pancreatic progenitor cells, forming organoids. The organoids retained the expression of pancreatic

progenitor markers (PDX1 and SOX9), epithelial marker (E-cad), internal polarization marker (mucin1), proliferative marker (pHH3), and endocrine differentiation marker (insulin). On the contrary, unconjugated PEG or stiffer PEG-LMN hydrogels (shear modulus > 1 kPa) were insufficient, demonstrating a loss of epithelial and pancreatic features. Notably, the authors did not present any comparative validation of these hydrogels' potency against the gold standard, Matrigel.

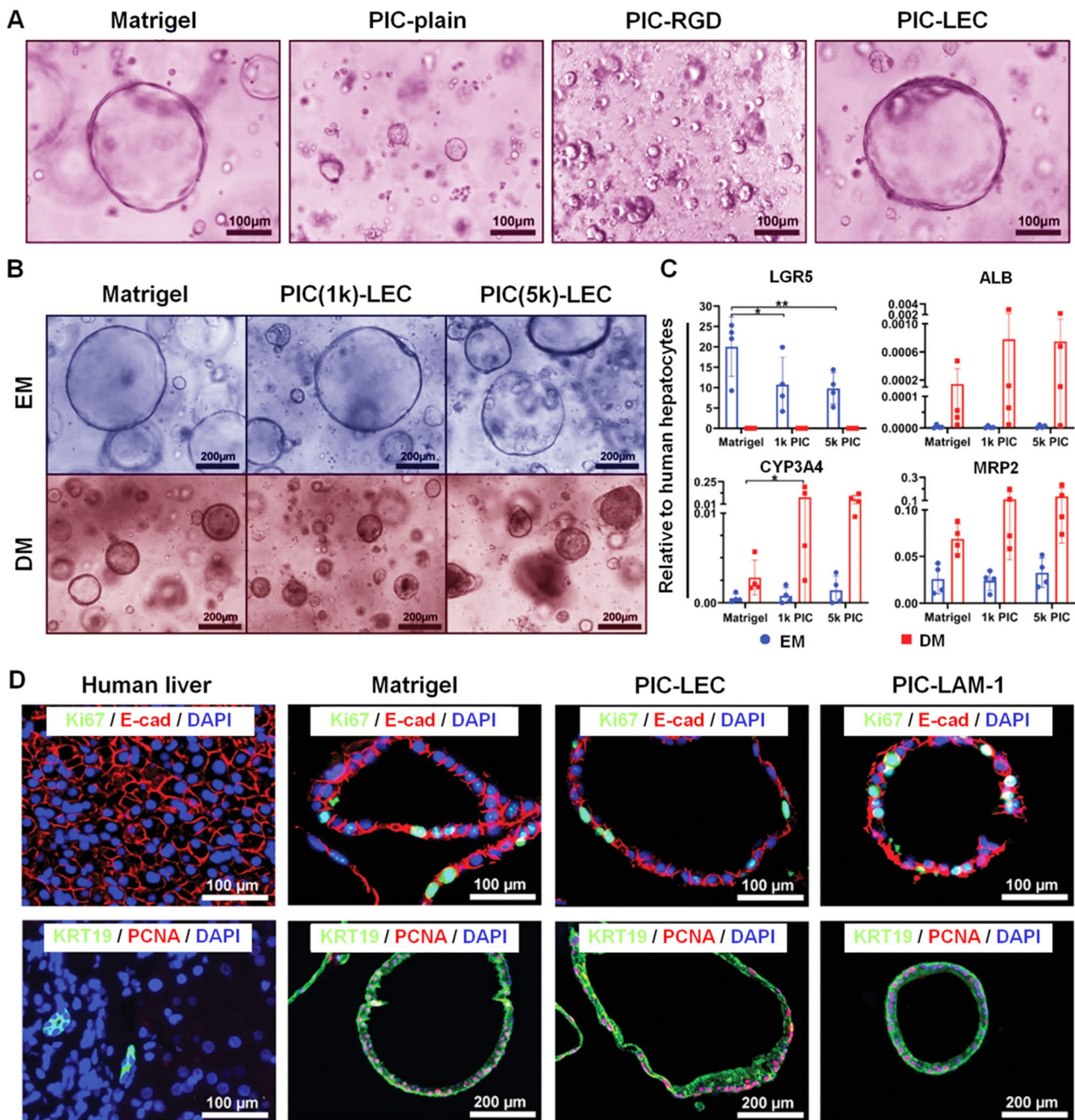


Fig. 5 a Representative light microscopy images of hepatic organoids, 7 days post-seeding, in Matrigel, PIC-plain, PIC-RGD, and PIC-LEC hydrogels; cultured in expansion medium. Organoids proliferated in Matrigel and PIC-LEC, but not in PIC-plain and PIC-RGD. Scale bar: 100 μ m. **b** Representative images of hepatic organoids in Matrigel and LEC-supplemented PIC hydrogels with different molecular weights—1 kDa (PIC(1 k)-LEC) or 5 kDa (PIC(5 k)-LEC); cultured in expansion and differentiation medium. Scale bar: 200 μ m. **c** Gene expression profiles of stem cells (LGR5) and hepatic markers (ALB, CYP3A4, and MRP2) in the organoids expanded or dif-

ferentiated in Matrigel, PIC(1 k)-LEC, and PIC(5 k)-LEC hydrogels; transcription levels normalized to human hepatocytes. Error bars: standard deviation (SD). “**” represents significant difference with p value ≤ 0.05 . **d** Representative immunofluorescence micrographs of hepatic organoids for epithelial (E-cad and cytokeratin 19 (KRT19)) and proliferative (proliferating cell nuclear antigen (PCNA) and Ki67) markers, cultured in Matrigel, PIC-LEC, and PIC-LMN-1. Nucleus was stained with DAPI. Native human liver tissue was taken as a control. Scale bars: 100 μ m (top), 200 μ m (bottom). Reproduced with permission from Ref. [75]. Copyright © 2020, Ye et al.

In a different study, hydrogel composed of Amikacin hydrate and poly(ethylene glycol) diglycidyl ether (PEGDE), formally termed as Amikagel, was employed as a substrate coating material to generate 3D islet organoids [105]. When cocultured with HUVEC on Amikagel, human ESC-derived pancreatic progenitor cells underwent spontaneous maturation and self-organization into functional organoids. The heterogenous organoids, thus formed, showed an enhanced

PDX1, insulin 1, and glucagon gene expression compared to those on Matrigel; the organoids also expressed C-peptide protein.

Besides, chemically defined hydrogels formed by RGD-modified SG dextran polymer and cross-linked with thiol-modified HA (together referred as DEX hydrogel) supported the formation and maintenance of human pancreatic organoids (from freshly isolated human pancreatic ducts) (Fig. 6)

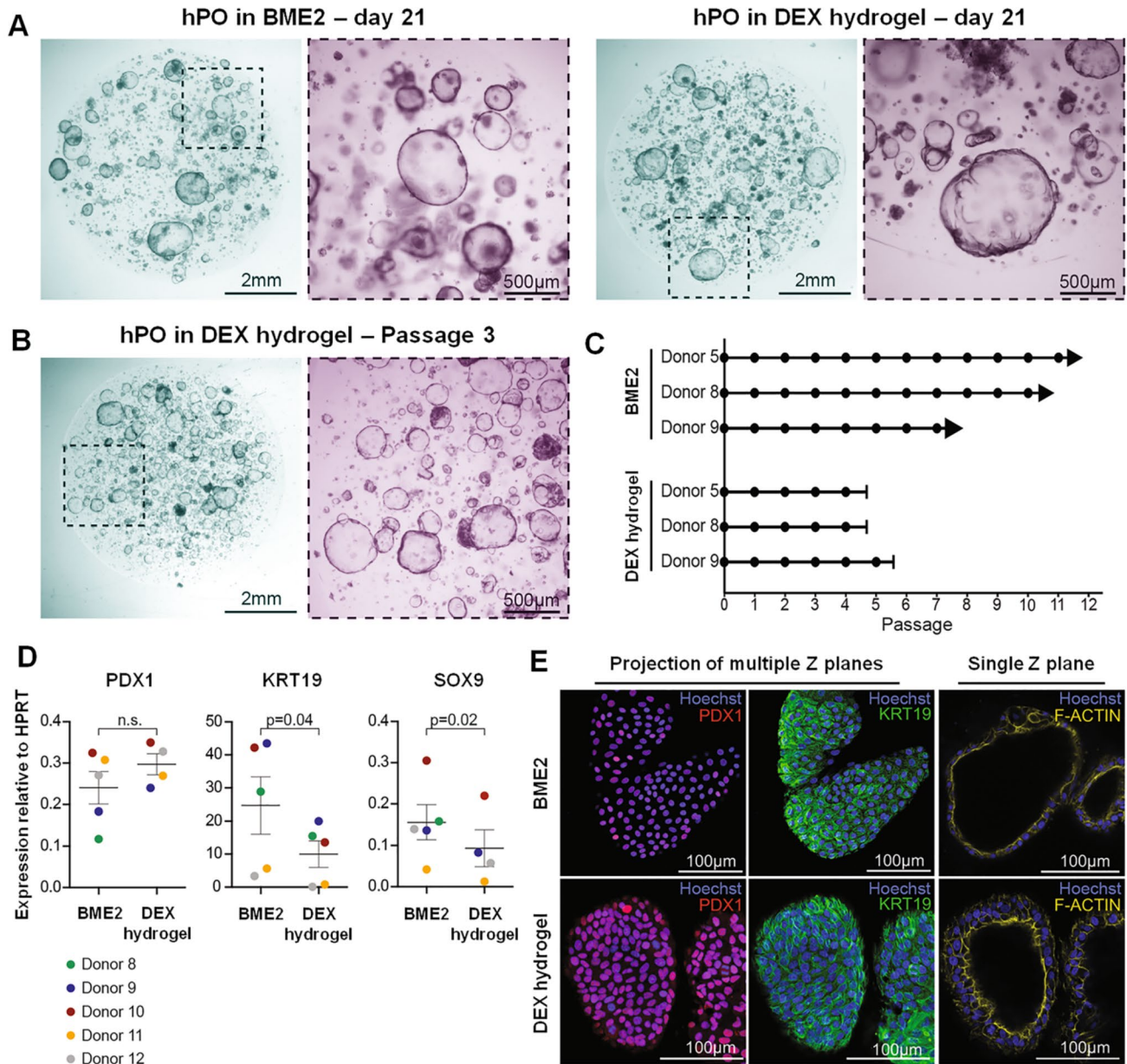


Fig. 6 **a** Bright-field micrographs of human pancreatic organoids in BME2 and DEX hydrogels after 21 days. DEX hydrogels were conjugated with minimal adhesion motif, RGD. Scale bars: 2 mm (left), 500 μ m (right). **b** Pancreatic organoids in DEX hydrogels at passage 3. Scale bars: 2 mm (left), 500 μ m (right). **c** Graphs demonstrating human pancreatic organoids derived from different donors, expanded

via passaging in BME2 and DEX hydrogels. **d** Gene expression profiling of pancreatic organoids derived from different donors in BME2 and DEX hydrogels. **e** Immunofluorescence staining of polarized pancreatic organoids in BME2 and DEX hydrogels. Nucleus was stained with Hoechst. Scale bars: 100 μ m. Reproduced with permission from Ref. [56]. Copyright © 2020, Georgakopoulos et al.

[56]. The sensitivity of DEX hydrogels toward dextranase allows easy passaging of pancreatic organoids. However, reduced expansion potential and limited passage numbers (up to passage 4, before cultures start to deteriorate), compared to Basement Membrane Extract Type 2 (BME2) matrix, highlight the need for further mechano-biochemical tuning of DEX hydrogels.

Renal organoids

The kidney is a bean-shaped organ, involved in the filtration of blood to remove wastes and control the body's fluidic and electrolytic balance. It consists of almost 20 different cell types, structured into the glomerulus, and proximal and distal tubules [106, 107]. Kidney organoids have witnessed widespread applicability in developmental biology, disease modeling, and drug screening [12, 108].

With the aim of studying renal tubulogenesis and evaluating drug-mediated nephrotoxicity, PEG and heparin-based hydrogels with tunable biochemical features (via the addition of heparin) and degradability (via incorporation of MMP-sensitive peptide) were reported (Fig. 7) [59]. Three different sets of hydrogels, namely degradable PEG-MMP-PEG (dPMP), non-degradable PEG-heparin (ndPH), and degradable PEG-MMP-heparin (dPMH) were prepared and evaluated parallelly to study the assembly process of human renal proximal tubule epithelial cells. The results revealed that dPMH hydrogels, over 4 weeks of culture, significantly promoted cellular organization into polarized renal tubules with a clear lumen, characterized by the presence of some cilia and microvilli at the luminal face. On the other hand, dPMP gels did not show any sign of polarization, while in ndPH gels, polarized spheroids with lumens filled with cellular debris were evident.

Another PEG-based hydrogel system, providing independent control over its mechanical features, tethered adhesion motif density, and hydrogel degradability, was employed to study epithelial morphogenesis [109]. The cysts formed under different formulation were scored in terms of their apicobasal polarity and lumen formation. Under optimal conditions, i.e., 4–4.5% PEG polymer density, 2 mM RGD peptide adhesion motif, and ~90% or more MMP-sensitive peptide threshold density (adjusted by replacing protease-degradable peptide with a slow degrading peptide variant), showed cyst growth, polarization, and lumenogenesis, similar to that observed in control collagen gels; hydrogels with altered properties resulted in abnormal morphogenesis.

Unlike the above studies, recent research revealed that the conjugation of MT1-MMP-sensitive IPES peptide to PEG hydrogels, instead of conventional MMP-sensitive peptide, was crucial for renal tubulogenesis [110]. Similarly, functionalization of RGD adhesion motif, but not collagen I-mimetic triple-helical peptide or LMN β 1 chain-derived

peptide, to the hydrogels efficiently supported renal tubulogenesis. PEG macromer size (10 or 20 kDa) and their polymeric density (together affecting the hydrogels' mechanical properties) were also shown to affect epithelial morphogenesis, thereby suggesting independent multi-tunability of these hydrogels.

Intestinal organoids

The intestine is the longest organ of the digestive tract and forms a major site of digestion, nutrient absorption, waste removal, and immune system homeostasis [93]. Anatomically, the intestinal epithelium is organized in a defined crypt/villus structure. Crypts contain intestinal stem cell niche that continuously divides to generate differentiated cells (enterocytes, goblet cells, enteroendocrine cells, Tuft cells, and Paneth cells), present on the villus unit [111, 112]. Intestinal organoids are among the first to be generated, and still, substantial research efforts have been focused on generating fully functional intestinal epithelium for investigating developmental processes, disease modelling, drug pharmacokinetics, and toxicity [73, 113–115].

A study demonstrated that defined, degradable PEG hydrogels conjugated with collagen I-mimetic triple-helical cell adhesion peptide, in addition to FN-binder peptide and COLIV-LMN binder peptide, and a cross-linker peptide with MMP- and sortase-sensitive sites, efficiently sustained the formation and differentiation of duodenal enteroids (Fig. 8) [74]. The generated undifferentiated enteroids appeared as cysts, expressing crypt-associated markers and evident proliferative capacity across passages, whereas, upon differentiation, markers of intestinal epithelium were observable. Moreover, alterations in the biomechanical features, caused by the change in polymeric density and size of PEG macromer (20 or 40 kDa or a combination of both) of the hydrogels, affected enteroid formation efficiency.

In the same milieu, to provide evidence toward the need for a dynamic environment for the maintenance of stem cell niche and organogenesis, soft PEG-RGD hydrogels were recently fabricated [115]. These hydrogels initially provided a stiff microenvironment that allowed maintenance and expansion of intestinal stem cells. Over the culture duration, hydrogels slowly underwent degradation, reducing the gel stiffness and promoting intestinal organogenesis. It is essential to mention that RGD adhesion motifs alone could suffice the stem cell niche maintenance; however, for organogenesis, supplementation of full-length LMN-111 protein was necessary. The non-degradable, static variants of the hydrogels could support cystogenesis and maintain leucine-rich repeat-containing G-protein-coupled receptor 5 (LGR5) positive intestinal stem cells even after repeated passaging but were incapable of inducing *in vitro* organogenesis. On

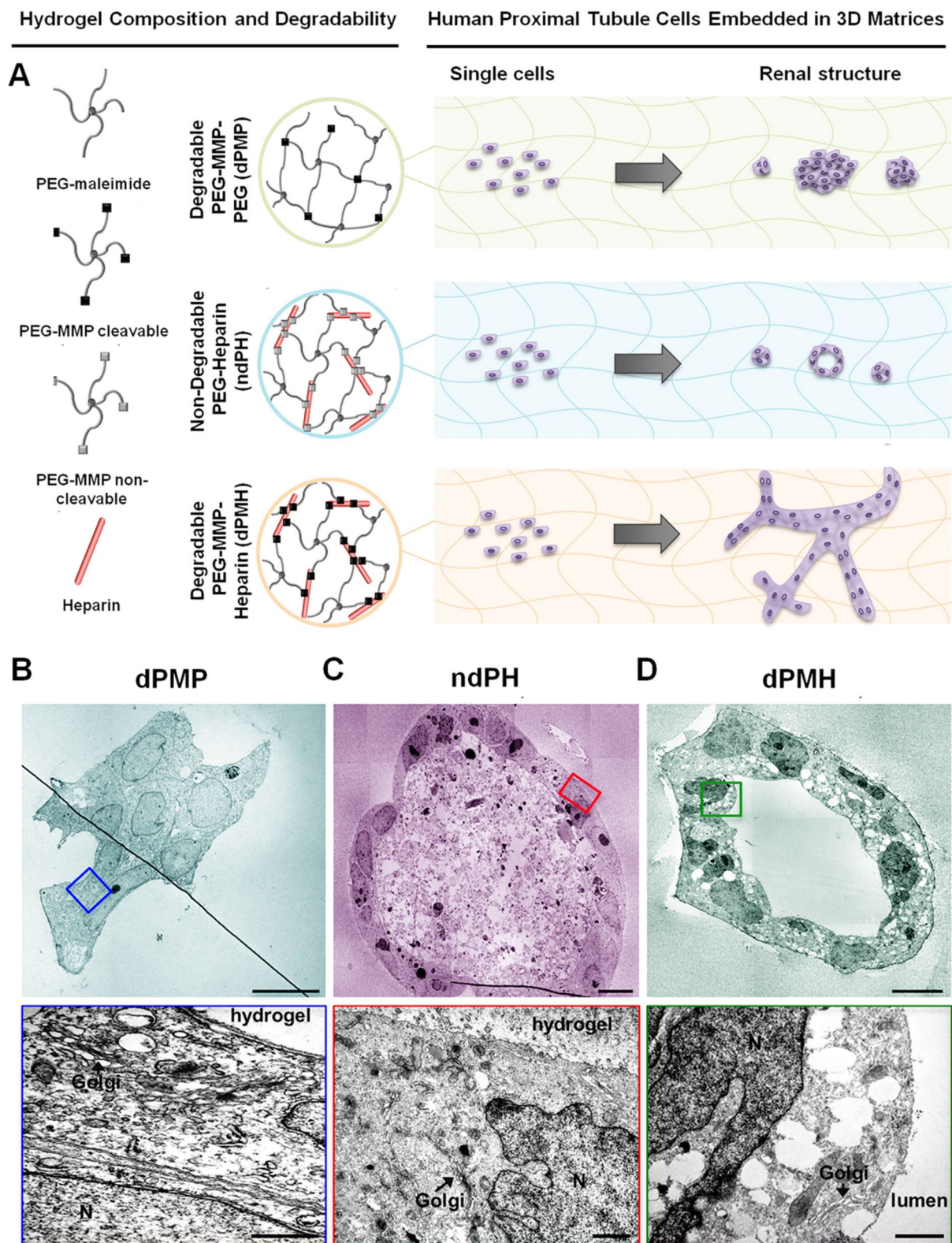


Fig. 7 a Schematic representation of chemically defined hydrogels with variable composition (PEG or heparin), degradability (MMP-sensitive or insensitive), and structural morphogenesis of human proximal tubule cells in different hydrogels. Electron micrographs of HK-2 cell-derived renal structures in **b** degradable PEG-MMP-PEG,

c non-degradable PEG-heparin, and **d** degradable PEG-MMP-heparin hydrogels (scale bar: 10 μm). Zoomed images have been provided below (scale bar: 1 μm). Golgi and N represent the Golgi apparatus and the nucleus, respectively. Reproduced with permission from Ref. [59]. Copyright © 2017, Elsevier B. V.

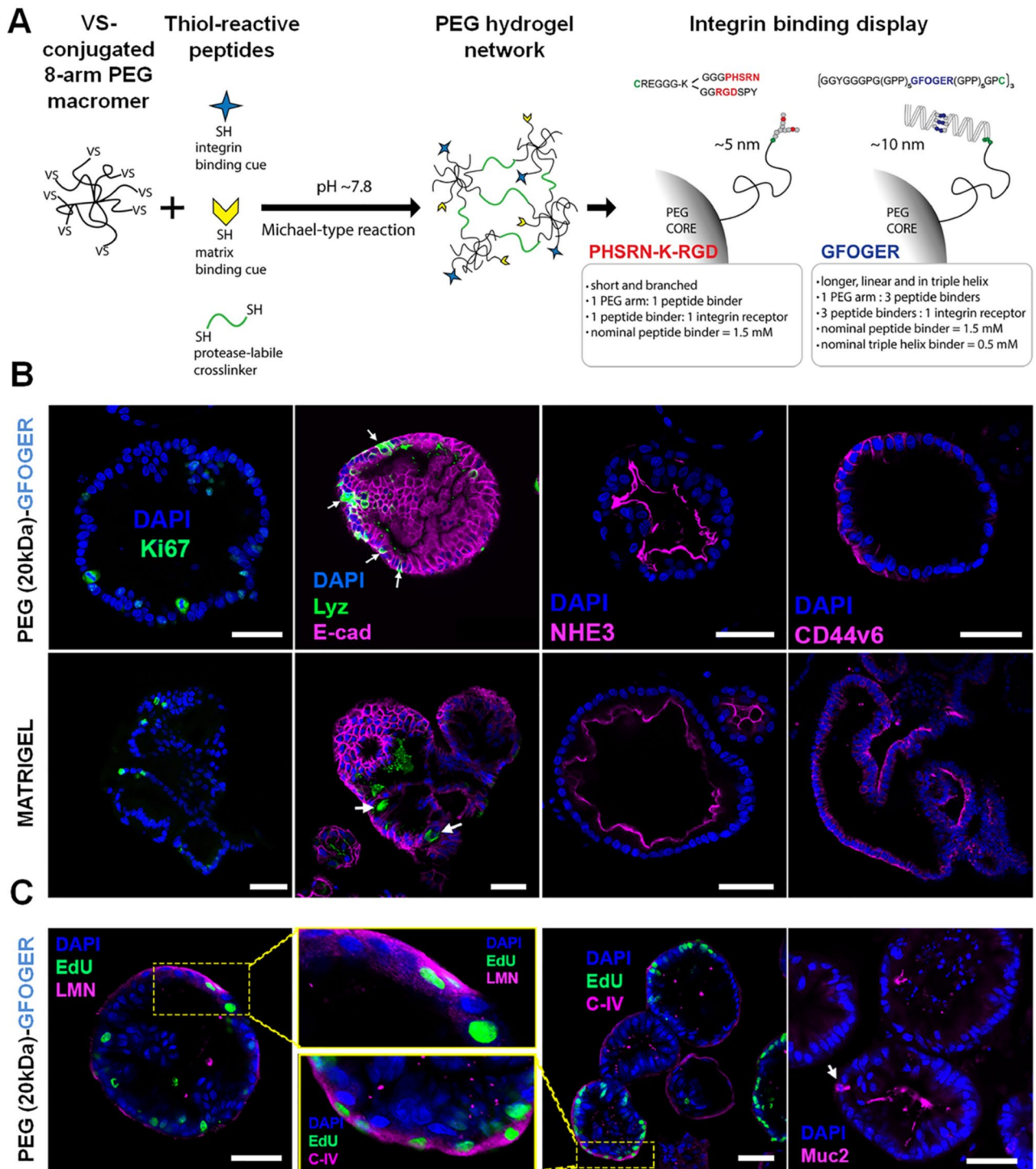


Fig. 8 **a** Schematic representation of assembling tunable, chemically defined, synthetic PEG hydrogel matrix. VS-conjugated 8-arm PEG macromers (20 or 40 kDa), in combination with thiol-reactive peptides, namely integrin-binding cues (PHSRN-K-RGD and GFOGER, with intrinsic affinity toward $\alpha 5\beta 1$ and $\alpha 2\beta 1$, respectively), matrix binding cues (FN-binding and COLIV-LMN binding), and protease-labile cross-linkers (MMP and sortase-sensitive), to form hydrogels via Michael-type reaction. The figure also highlights branched (PHSRN-K-RGD) and triple-helical (GFOGER) conformation of the

integrin-binding peptides, bound to the PEG arm. **b, c** Representative immunostained polarized 10-day-old intestinal organoids in Matrigel and PEG (20 kDa)-GFOGER hydrogel demonstrating proliferative cells (EdU, Ki67), mature enterocytes (sodium-hydrogen exchanger 3, NHE3), goblet (mucin 2, Muc2), Paneth (lysozyme, Lyz), epithelial (E-cad), and basolateral (LMN, COLIV, and CD44-v6) markers. Nucleus was stained with DAPI. Scale bar 50 μ m. Reproduced with permission from Ref. [74]. Copyright © 2020 Elsevier B. V.

the other hand, the fast degrading variants generated lesser cysts with lower LGR5+ stem cell population.

Alternatively, natural biomaterials have also been used for culturing intestinal organoids. For instance, alginate hydrogels (concentration 1%, storage modulus ~ 78 Pa) were shown to sustain the growth of human intestinal organoids derived from human ESC or iPSC lines; however, the yield of organoids was significantly lower than in the case of Matrigel [64]. Interestingly, alginate-grown organoids showed polarized architecture with the expression of different intestinal epithelial differentiation markers, similar to those grown in Matrigel. Upon *in vivo* implantation organoids underwent maturation, closely resembling the native human intestinal tissue. Another defined hydrogel composition of fibrin (concentration 3.5–4 mg/mL, storage modulus ~ 77–140 Pa) supplemented with LMN (2 mg/mL) promoted the formation, growth, and epithelial morphogenesis of the intestinal organoids, similar to Matrigel (Fig. 9) [52]. Supplementation of other ECM components, namely COLIV and heparin, were insufficient for the purpose, highlighting the critical role of LMN in intestinal morphogenesis.

Other organoids

Apart from the above-discussed ones, chemically defined hydrogels could also sustain organoids' growth associated with other tissues/organs.

The mammary gland is a branched tubular organ that undergoes two distinct developmental phases: (i) embryonic and (ii) postnatal during puberty and pregnancy; to study this, organoid models are often preferred [116]. Besides, their widespread applicability in breast cancer biology cannot be disregarded. Recently, soft, degradable, and chemically defined PEG-heparin hydrogels were shown to promote morphogenesis of non-transformed mammary epithelial cells into polarized multicellular organoids with a clear lumen, resembling terminal ductal lobular units (acini), with growth characteristics similar to those in Matrigel [60]. The cells in non-degradable variants also formed cysts but had lower lumen clearance, while the cells in stiffer variants exhibited higher proliferation, lower polarization, and invasive features.

Endometrium, the inner lining of the uterus, comprising epithelial and mesenchymal cells, is subjected to periodic alterations in growth, differentiation, and degradation under the influence of ovarian hormones [117]. Endometrial organoids have emerged as potential candidates for recapitulating these periodic changes and endometrium-associated pathological issues. In this regard, fully synthetic matrices coupled with collagen I-mimetic triple-helical cell adhesion peptide, FN-binder peptide, COLIV-LMN binder peptide, and a cross-linker peptide with MMP- and sortase-sensitive sites could provide necessary cues to generate polarized

endometrial organoids with EdU+ and EpCAM+ proliferative and differentiated epithelial cells, similar to that of Matrigel (Fig. 10) [74].

The immune system is highly intricate and is still one of the most challenging systems to study. In order to recapitulate such complex microenvironment, lymph node organoids were developed in MMP-sensitive, defined PEG hydrogels using Naïve B cells and 40LB stromal cells (genetically modified to express CD40 ligand and produce B cell-activating factor) [118]. The study revealed that maleimide group, but not vinyl sulfone and acrylate, when used as end-group functionality in PEG hydrogels, sustained B cells' survival and germinal center-like induction. Moreover, incorporating collagen I-mimetic peptide, similar to that present in the niche, promoted germinal center-like dynamics and epigenetics; peptides mimicking FN/vitronectin and VCAM1 were insufficient for the purpose.

Bone marrow is a soft, spongy tissue inside the bones, wherein hematopoietic stem and progenitor cells (HSPCs) and bone marrow stromal cells (BMSCs) reside and contribute in sustained repair and regeneration of the body. Developing a highly controlled microenvironment for studying the cellular dynamics in the bone marrow is challenging. In this regard, bone marrow organoids were formed in a tunable and defined PEG-HA composite hydrogels [92]. Hydrogels were hydrolytically sensitive to MMP peptide and were conjugated with RGD motif. The study revealed that the hydrogels could maintain, expand, and differentiate human HSPCs and BMSCs *in vitro*. Additionally, PEG hydrogels coupled with 20 different cell-instructive peptide moieties (including a set of integrin-binding and MMP-sensitive domains of marrow-specific ECM proteins) and native bone marrow-mimetic mechanical properties can also be employed for generating bone marrow organoids [119].

Tables 2 and 3 summarize current developments in chemically defined hydrogels from natural and synthetic materials for organoid culture, respectively.

Conclusion and outlook

The capacity of organoids to recapitulate and reflect the intricacies of native tissue and organs has led to their potential applications in biomedical and pharmaceutical industries. Over the years, Matrigel continues to be the most suitable platform for a myriad of organoid-based applications. Alternatively, recent interventions have highlighted a similar potency of decellularized tissue-derived ECM for organoid generation. However, the lack of spatiotemporal control over their tunable characteristics limits their translational aspects, calling upon the need to explore advanced platforms.

Chemically defined matrices, involving the use of natural, synthetic materials or their biohybrids, offer tailoring

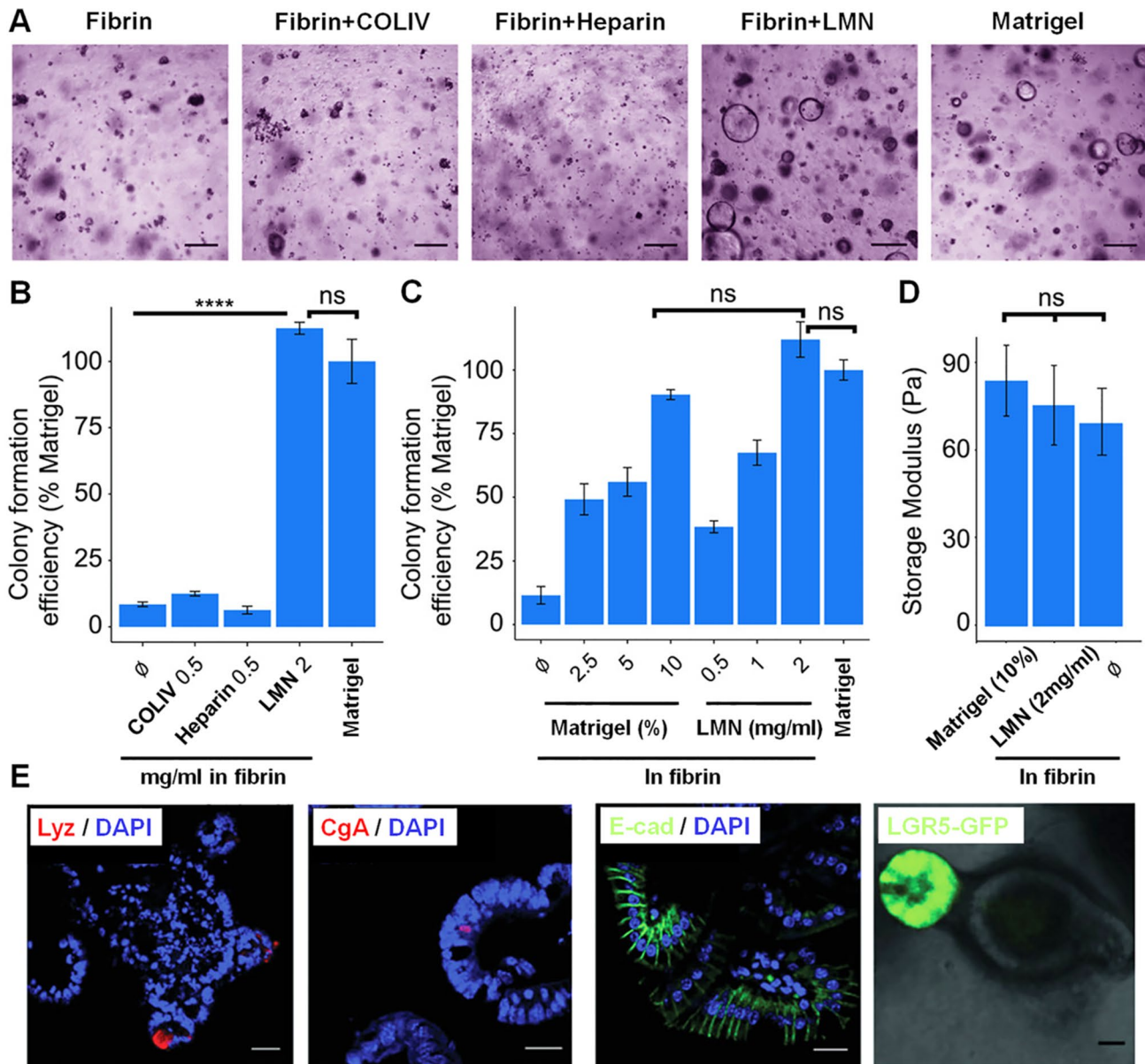


Fig. 9 **a** Bright-field micrographs, showing morphogenesis of mouse small intestinal stem cells in pure Matrigel or fibrin hydrogels (pure or supplemented with COLIV, heparin, and LMN). Scale bar 200 μ m. **b** Quantitative analysis of colony formation efficiency of mouse small intestinal stem cells under different supplementation of fibrin hydrogels normalized to pure Matrigel. Error bars: SD. **c** Quantitative analysis of colony formation efficiency of mouse small intestinal stem cells in fibrin hydrogel supplemented with varying concentration of Matrigel or LMN, normalized to Matrigel. Error bars: SD. **d**

Quantification of mechanical properties of pure and supplemented fibrin hydrogels. Error bars: SD. **e** Representative images of intestinal organoid sections stained for Lyz (Paneth cells), chromogranin A (CgA, enteroendocrine cells), E-cad (epithelial cells), and LGR5-GFP (intestinal stem cells). Paneth and intestinal stem cells were exclusively present in the crypt-like domains. Nucleus was stained with DAPI. Scale bar: 20 μ m. Reproduced with permission from Ref. [52]. Copyright © 2018, Broguiere et al. Published by WILEY-VCH Verlag GmbH & Co. KGaA, Weinheim

advantages over biochemical, mechanical, and degradation-related features, thereby guiding the generation, expansion, differentiation, and maturation of organoids in a reproducible manner, as highlighted in the present work (Fig. 11). Further expansion in the organoid technology needs a critical upgradation from the archaic cell culture regimes and

a better understanding of cellular responses upon interaction with different biointerfacial cues. The contact printing technology or combinatorial approaches, wherein different compositions of ECM proteins or bioactive peptides could be spotted on a hydrogel platform (maybe of variable stiffness), can turn out to be handy, ascertaining their influence

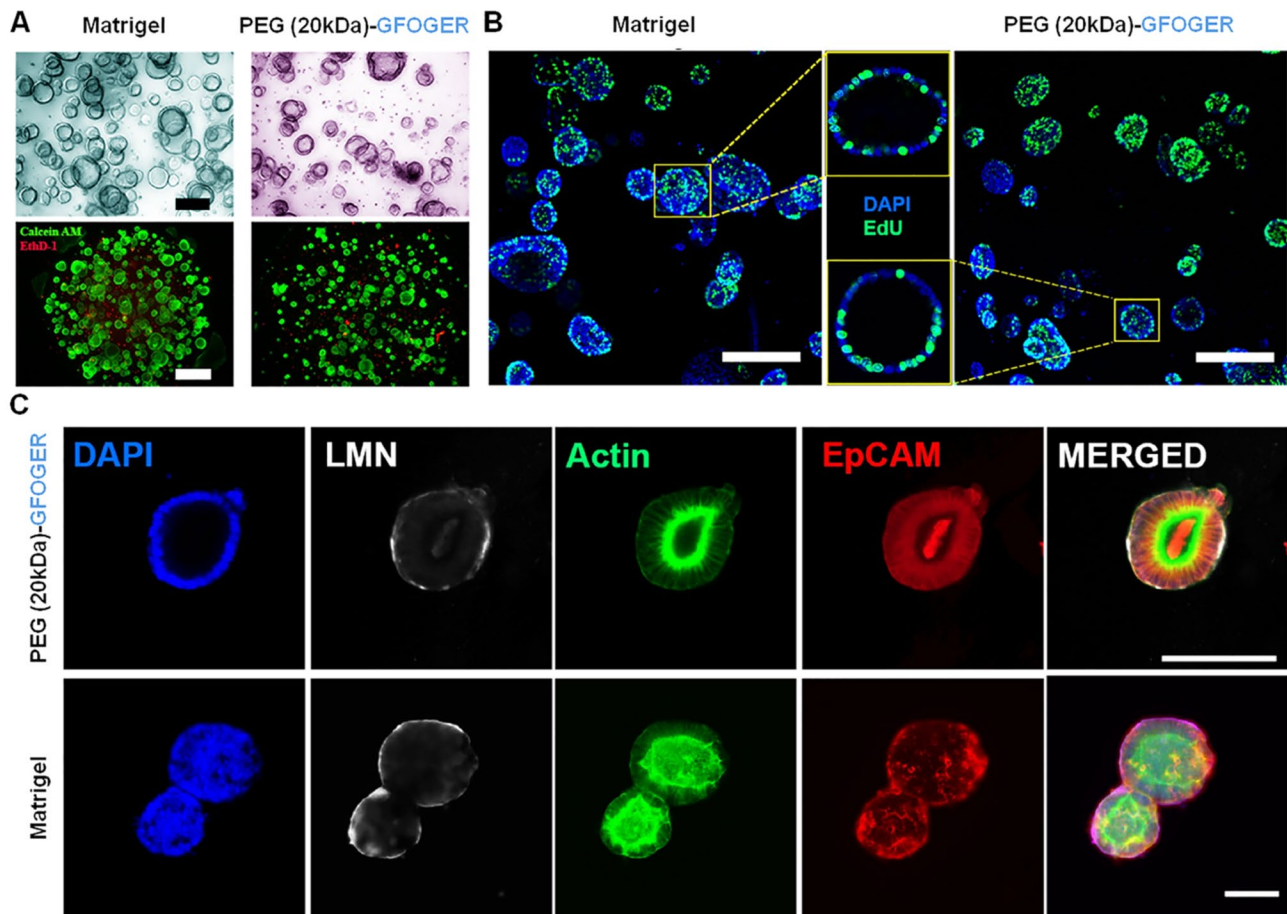


Fig. 10 **a** Representative bright-field and corresponding live/dead images of endometrial organoids in Matrigel and PEG (20 kDa)-GFOGER hydrogels. Scale bars: 200 μm (top), 500 μm (bottom). **b**, **c** Immunostained endometrial organoids in Matrigel and PEG (20 kDa)-GFOGER demonstrating proliferative cells (EdU+), api-

cal (actin+), basolateral (LMN+), and epithelial (EpCAM+) markers. Scale bar 200 μm (**b**) and 100 μm (**c**). Nucleus was stained with DAPI. Reproduced with permission from Ref. [74]. Copyright © 2020, Elsevier B. V.

on phenotypic characteristics of either stem cells or progenitor cell population [130, 131].

Further impactful development in this domain can be attributed to (i) synthetic hydrogels that are fully or partially cross-linked by physical interactions, or (ii) photomutable-synthetic hydrogels [29, 132–135]. In contrast to chemically cross-linked hydrogels, physically cross-linked ones are more dynamic and exhibit a broader sensitivity to the surrounding environment. The use of photomutable-synthetic hydrogels also offers targeted dynamic tuning of matrix mechanics or generating a local display of growth factors via light and photo-cleavable components attached to the matrix.

However, for research progress, a fruitful collaboration between material scientists, biologists, engineers, and

clinicians across academia and industry, aiming toward popularization and improvement in these defined platforms, is necessary. It is also essential to ensure the availability and finding strategies for easy, user-friendly usage of these platforms among the practitioners. At the commercial level, QGel, a start-up company, is making an effort to meet the demand of chemically defined synthetic matrices for a wide range of organoid-related applications (<https://www.qgel.com/>).

Besides, organoids related to many tissues, including cardiac and retinal, have still not been reported in chemically defined hydrogels, presenting another scope for future development in this sphere.

On a concluding note, we upbeat that dedicated effort in this direction can open up new vistas in generating clinically compatible organoid tissue models in the near future.

Table 2 Chemically defined hydrogels from natural biomaterials and their derivatives for organoid culture

S. No.	Organoid type	Polymer	Peptide sequence (function)	Tunable features (if reported)	Mechanical properties	Cells used	Control matrices	References
1	Cerebral	HA and protonated chitosan	NA	NA	Young's modulus: 9.8 kPa	Human iPSCs	NA	[67]
2	Neural	Thiolated heparin and HA methacrylate	NA	Biochemical features	Storage modulus: 0.3 (soft) and 1.17 kPa (rigid)	hiPSK3 cells	Geltrex	[120]
3	Pancreatic	SG dextran (thiol-reactive) and thiol-modified HA	RGD	NA	NA	Pancreatic duct/pre-established organoid fragments	BME-2	[56]
4	PDAC	Collagen	NA	NA	NA	PDAC cancer PDX	NA	[44]
5	Liver	Cellulose	NA	Mechanical features	Young's modulus: 0.255 kPa	Pre-established human liver organoid	Matrigel	[102]
6	Liver	Fibrin, alginate, chitosan	NA	Biochemical features	NA	iHeps	NA	[53]
7	Colorectal	Gelatin-phenol and HA-phenol	NA	Mechanical and biochemical features	Young's modulus: 14.6 kPa	Colorectal cancer PDX	Geltrex	[121]
8	Intestinal	Alginate	NA	NA	NA	Pre-established human intestinal organoid	Matrigel	[45]
9	Intestinal	Alginate	NA	Mechanical features	Storage modulus: < 0.1 kPa	Human ESC/iPSC lines	Matrigel	[64]
10	Intestinal	Collagen	NA	NA	NA	Pre-established human intestinal organoid	Matrigel	[46]
11	Intestinal	Collagen	NA	NA	NA	Human crypt fragments and intestinal subepithelial myofibroblasts	Matrigel	[47]
12	Intestinal	Collagen	NA	Mechanical features	Storage modulus: 0.029 kPa	Mouse crypt fragments	NA	[122]
13	Intestinal	Fibrin and LMN	NA	Mechanical and biochemical features	Storage modulus: 0.077 kPa	Mouse small intestinal stem cells	Matrigel	[52]

BME-2, Basement Membrane Extract Type 2; PDAC, pancreatic ductal adenocarcinoma; PDX, patient-derived xenograft; hiPSCs, human-induced pluripotent stem cells; hESCs, human embryonic stem cells; iHeps, hiPSCs-derived hepatocyte-like cells; NA, not available

Table 3 Chemically defined hydrogels from synthetic biomaterials and their derivatives or biohybrids for organoid culture

S. No.	Organoid type	Polymer	Conjugated peptide sequence	Conjugated peptide source/function	Peptide conjugation strategy	Tunable features (if reported)	Mechanical properties	Cells	Control matrices	References
1	Cerebellar	PEG-8MAL	CG(PKG) ₄ (POG) ₄ (DOG) ₄ CG(PKG) ₄ (POG) ₄ (DOG) ₄ -RGDSPG	Collagen-like peptide Collagen-like peptide with cell adhesion motif	Thio–maleimide “click” chemistry	Biochemical features	Young’s modulus: 80.1 kPa Young’s modulus: 61.2 kPa	Cerebellar neuronal–glial cell	–	[95]
2	Neural	PEG-8NB	CRGDS KCGG-PQGIWG-QGCK	Cell adhesion motif MMP-sensitive peptides	Thio–Norbornene “click” chemistry	Mechanical and biochemical features	NA	Human ESC-NPCs, MSCs, pericytes, endothelial cells, and microglia precursors	–	[123]
3	Neural	PEG-8VS	FKGG-GDQGIAGF-ERCG NQEQVSPL-ERCG	MMP-insensitive, lysine-donor transglutaminase factor XIIIa substrate peptide Glutamine-acceptor transglutaminase factor XIIIa substrate peptide	Thio–vinyl sulfone “click” chemistry	–	–	mESCs	Matrigel	[124]

Table 3 (continued)

S. No.	Organoid type	Polymer	Conjugated peptide sequence	Conjugated peptide source/function	Peptide conjugation strategy	Tunable features (if reported)	Mechanical properties	Cells	Control matrices	References
4	Neutral	PEG-8VS	FKGG-VPMSMRGG-ERCG FKGG-GDQGIAGF-ERCG	MMP-sensitive, lysine-donor transglutaminase factor XIIIa substrate peptide MMP-insensitive, lysine-donor transglutaminase factor XIIIa substrate peptide	Thiol–vinyl sulfone "click" chemistry	Mechanical features, degradability, and biochemical features	Young's modulus: 2–4 kPa	Mouse ESCs	Matrigel	[94]
5	Pancreatic	Amikacin hydrate and PEGDE	NQEQVSPL-ERCG	Glutamine-acceptor transglutaminase factor XIIIa substrate peptide	–	Mechanical features	Young's modulus: 300 kPa	Human ESC-PP with HUVEC	Matrigel	[105]
6	Pancreatic	PEG-VS (with LMN)	FKGG-GPQGIWGQ-ERCG NQEQVSPL-ERCG	MMP-sensitive, lysine-donor transglutaminase factor XIIIa substrate peptide Glutamine-acceptor transglutaminase factor XIIIa substrate peptide	Thiol–vinyl sulfone "click" chemistry	Mechanical and biochemical features	Shear modulus: 0.25 kPa	Embryonic pancreas progenitor cells	Matrigel	[104]

Table 3 (continued)

S. No.	Organoid type	Polymer	Conjugated peptide sequence	Conjugated peptide sequence	Conjugated peptide source/function	Peptide conjugation strategy	Tunable features (if reported)	Mechanical properties	Cells	Control matrices	References
7	Intestine	PEG-4MAL	GRGDSPC	CGGRKRLQQLSIRT	Cell adhesion motif (FN or vitronectin mimic) LMN α 1 chain-derived (AG73 peptide)	Thiol–maleimide "click" chemistry	Polymer density and biochemical features	Storage modulus: < 0.1 kPa	Human iPSCs	Matrigel	[73]
			GYGGG(GPP) ₅ GPC	GYGGG(GPP) ₅ GFOGER(GPP) ₅ GPC	Collagen I-mimetic triple-helical peptide						
			CGGAASIKVAVSADR	CGGAASIKVAVSADR	LMN α 1 chain-derived						
			GCRD-GPQGIWGQ-DRCG	GCRD-GPQGIWGQ-DRCG	Protease-degradable peptide (collagen-derived)						

Table 3 (continued)

S. No.	Organoid type	Polymer	Conjugated peptide sequence	Conjugated peptide source/function	Peptide conjugation strategy	Tunable features (if reported)	Mechanical properties	Cells	Control matrices	References
8	Intestinal	PEG-8VS and PEG-8Act	FKGG-GPQGIWGQ-ERCG FKGG-GDQGIAGF-ERCG	MMP-sensitive, lysine-donor transglutaminase factor XIIIa substrate peptide MMP-insensitive, lysine-donor transglutaminase factor XIIIa substrate peptide	Thiol-vinyl sulfone "click" chemistry	Mechanical features, tethered adhesion motif density, hydrogel degradability, and biochemical features	Shear modulus: 1.3 kPa	Mouse crypt fragments or mouse intestinal stem cells	Matrigel	[91, 115]
			NQEQVSPL-ERCG	Glutamine-acceptor transglutaminase factor XIIIa substrate peptide						
			NQEQVSPL-RGDSPG	Glutamine-acceptor transglutaminase factor XIIIa substrate peptide with RGD motif						
9	Intestine	Dibenzylcyclooctyne-functionalized 4-arm PEG with azide-functionalized cross-linkers	Azide-functionalized RGD	Cell adhesion motif	Strain-promoted azide-alkyne cycloaddition (SPAAC) reaction	Polymer density and hydrogel photodegradability	Storage modulus: < 1.5 kPa	Single cells from pre-established small intestinal organoids	–	[125]

Table 3 (continued)

S. No.	Organoid type	Polymer	Conjugated peptide sequence	Conjugated peptide source/function	Peptide conjugation strategy	Tunable features (if reported)	Mechanical properties	Cells	Control matrices	References
10	Intestinal	QGel CN99 (Proprietary formulation)	–	–	–	–	Shear modulus: 0.45 kPa (tends to reduce to 0.01–0.05 Pa upon culture)	Colonic crypt-derived single cells	Matrigel	[126]
11	Intestinal	Polypeptide chain-based hydrogels	–	–	–	Mechanical and biochemical features	Storage modulus: 0.18 (soft) and 1.22 kPa (rigid)	Mouse intestinal tissue fragments	Collagen I	[114]
12	Intestinal	PEG-4MAL	GRGDSPC	Cell adhesion motif (FN or vitronectin mimic)	Thio–maleimide "click" chemistry	Mechanical and biochemical features	Storage modulus: 0.1 kPa	Human iPSCs	Matrigel	[90]
			GCRDGPQGIWQDRCG	Protease-degradable peptide (collagen-derived)						
13	Intestinal	PEG-8VS	GGYGGG PG(GPP) ₅ GFOGER(GPP) ₅ GPC PHSRNNGGK-(GGG-ERCG)- GGRGDSPY GCRD-VPMSMRGG-DRCG GCRE-TLQPVYEMVGV GCRE-ISAFLGIPFAEPPMG- PRRFLPPEPKKP	Collagen I-mimetic triple-helical peptide FN-derived cell adhesion peptide MMP-sensitive peptide FN-binding peptide COLIV and LMN binding peptide	Thio–vinyl sulfone "click" chemistry	Mechanical features, tethered adhesion motif density, and biochemical features	Storage modulus: 0.81–0.93 kPa	Pre-established organoid fragments	Matrigel	[74]

Table 3 (continued)

S. No.	Organoid type	Polymer	Conjugated peptide sequence	Conjugated peptide source/function	Peptide conjugation strategy	Tunable features (if reported)	Mechanical properties	Cells	Control matrices	References
14	Endometrial	PEG-8VS	GGYGGG PG(GPP) ₅ GFOGER(GPP) ₅ GPC PHSRNNGGK-(GGG-ERCG)- GGRGDSFY GCRD-LPRTG-GPQGIAGQ- DRCG GCRE-TLQPVYEVYMGV GCRE-ISAFLGIPFAEPPMG- PRRFLPPEPKKP	Collagen I-mimetic triple-helical peptide FN-derived cell adhesion peptide MMP-sensitive peptide with sortase-sensitive recognition site FN-binding peptide COLIV and LMN binding peptide	Thiol–vinyl sulfone "click" chemistry	Biochemical features	Storage modulus: 0.81–0.93 kPa	Pre-established organoid fragments	Matrigel	[74]

Table 3 (continued)

S. No.	Organoid type	Polymer	Conjugated peptide sequence	Conjugated peptide source/function	Peptide conjugation strategy	Tunable features (if reported)	Mechanical properties	Cells	Control matrices	References
15	Liver	PEG-8VS	FKGG-GPQGIWGQ-ERCG	MMP-sensitive, lysine-donor transglutaminase factor XIIIa substrate peptide	Thiol–vinyl sulfone "click" chemistry	Mechanical features, degradability, and biochemical features	Storage modulus: 0.3 (soft) and 1.3 kPa (rigid)	Mouse biliary duct fragments	Collagen I and Matrigel	[101]
			FKGG-GDQGIAGF-ERCG	MMP-insensitive, lysine-donor transglutaminase factor XIIIa substrate peptide						
			NQEQVSPL-ERCG	Glutamine-acceptor transglutaminase factor XIIIa substrate peptide						
			NQEQVSPL-RGDSPG	Glutamine-acceptor transglutaminase factor XIIIa substrate peptide with RGD motif						
16	Liver	PEG-8VS (with gelatin); supplemented with either LMN-111 or LMN-521	NQEQVSPL-ERCG	Glutamine-acceptor transglutaminase factor XIIIa substrate peptide	Thiol–vinyl sulfone "click" chemistry	Mechanical and biochemical features	Compressive modulus: 2.6 kPa	Pre-established organoid fragments	Matrigel	[127]

Table 3 (continued)

S. No.	Organoid type	Polymer	Conjugated peptide sequence	Conjugated peptide source/function	Peptide conjugation strategy	Tunable features (if reported)	Mechanical properties	Cells	Control matrices	References
17	Liver	PIC azide supplemented with either LEC or human recombinant LMN-111	Dibenzocyclooctyne-conjugated GRGDS	Cell adhesion motif	CuAAC "click" chemistry	Mechanical and biochemical features	Storage modulus: 0.012 (1 kDa weight) and 0.038 kPa (5 kDa weight)	Single cells from pre-established liver organoids	Matrigel	[75]
18	Renal	PEG-4MAL, Heparin-MAL	GCGGPGQGWGGCG	MMP-sensitive peptide	Thiol–maleimide "click" chemistry	Hydrogel degradability and biochemical features	Storage modulus: 0.5 kPa	Human renal proximal tubule cells	Matrigel	[59]
19	Renal	PEG-4MAL, Heparin-MAL	GRGDSPC GYGGP(GPP) ₅ GFOGER (GPP) ₅ GPC CGGEGYEGYIGSR GCRD-IPESLRAG-DRCG	Cell adhesion motif (FN or vitronectin mimic) Collagen I-mimetic triple-helical peptide LMN β 1 chain-derived MT1-MMP-sensitive cross-linking peptide IPES Protease-degradable peptide (collagen-derived)	Thiol–maleimide "click" chemistry	Mechanical features, tethered adhesion motif density, hydrogel degradability, and Biochemical features	Storage modulus: 0.2 kPa	Immortalized mouse inner medullary collecting duct and mouse renal proximal tubule cells	Matrigel	[110]
20	Renal	PEGDA, Thiolated HA	NA	NA	NA	NA	NA	Mouse proximal tubules	NA	[128]
21	Mammary gland	PEG-4MAL, Heparin-MAL	GCGGPGQGWGGCG GCGIGQQGPWGGCG	MMP-sensitive peptide MMP-insensitive peptide	Thiol–maleimide "click" chemistry	Mechanical features, hydrogel degradability, and biochemical features	Storage modulus: 0.2–0.35 kPa	MCF10A cell line	Matrigel	[60]

Table 3 (continued)

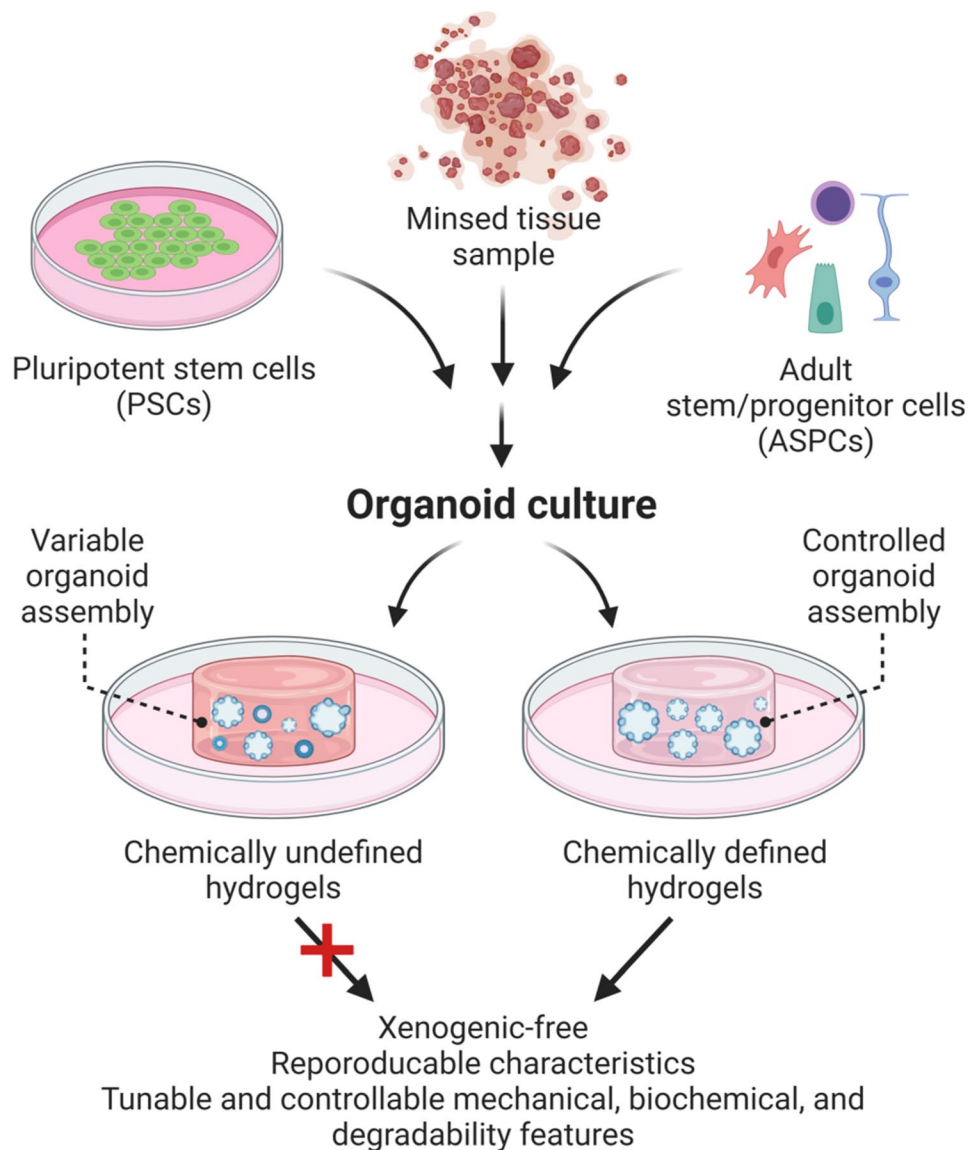
S. No.	Organoid type	Polymer	Conjugated peptide sequence	Conjugated peptide source/function	Peptide conjugation strategy	Tunable features (if reported)	Mechanical properties	Cells	Control matrices	References
22	Mammary gland	PIC azide	Dibenzocyclooctyne-conjugated GRGDS	Cell adhesion motif	CuAAC "click" chemistry	Mechanical and biochemical features	Storage modulus: 0.3 kPa	Mouse mammary gland fragments or epithelial cells	Matrigel	[69]
23	Prostate	PIC azide	Dibenzocyclooctyne-conjugated GRGDS	Cell adhesion motif	CuAAC "click" chemistry	Mechanical and biochemical features	Storage modulus: 0.3 kPa	Mouse prostate epithelial cells	Matrigel	[69]
24	Bone marrow	PEG-8VS and vinyl sulfonated HA	FKGG-RGDSPG FKGG-GPQGIWGQ-ERCG NQEVSPL-ERCG	Cell adhesion motifs MMP-sensitive, lysine-donor transglutaminase factor XIIIa substrate peptide Glutamine-acceptor transglutaminase factor XIIIa substrate peptide	Thiol-vinyl sulfone "click" chemistry	Biochemical features and hydrogel degradability	Storage modulus: 0.25–0.32 kPa	Human BMSCs and CD34+ hHSPC	NA	[92]
25	Lymphoma	PEG-4MAL	GRGDSPC GREDVGC GCRD-VPMSMRGG-DRCG	Cell adhesion motif (FN or vitronectin mimic) Cell adhesion motifs (VCAM1 mimic) MMP-sensitive peptide	Thiol-maleimide "click" chemistry	Biochemical features	NA	Human tonsil-derived FDCs HK, HBL-1, OCI-Ly10, OCI-Ly12, and HuT-78 cells	NA	[129]

Table 3 (continued)

S. No.	Organoid type	Polymer	Conjugated peptide sequence	Conjugated peptide source/function	Peptide conjugation strategy	Tunable features (if reported)	Mechanical properties	Cells	Control matrices	References
26	Immune	PEG-4MAL or PEG-4VS or PEG-4Act	GRGDSPC GREDEVGC	Cell adhesion motif (FN or vitronectin mimic) Cell adhesion motifs (VCAM1 mimic)	Thiol-ene "click" chemistry (depending upon the reacting groups)	Hydrogel degradability and biochemical features	NA	40LB stromal cells (genetically modified from NIH/3T3 fibroblasts to express CD40 ligand and produce B cell-activating factor) and mouse B cells	NA	[118]
			GYGGG(GPP) ₅ GFOGER(GPP) ₅ GPC	Collagen I-mimetic triple-helical peptide						
			GCRD-VPMSMRGG-DRCG	MMP-sensitive peptide						

CuAAC, copper-assisted azide-alkyne cycloaddition; PEG-4MAL, 4-arm PEG macromer with terminal maleimide groups; PEG-8MAL, 8-arm PEG macromer with terminal maleimide groups; PEG-8NB, 8-arm PEG macromer with terminal norbornene groups; PEG-8VS, 8-arm PEG macromer with terminal vinyl sulfone groups; PEG-4VS, 4-arm PEG macromer with terminal vinyl sulfone groups; PEG-4Act, 4-arm PEG macromer with terminal acrylate groups; PEG-8Act, 8-arm PEG macromer with terminal acrylate groups; ESC-DE, ESCs-derived definite endoderm; ESC-PP, ESCs-derived pancreatic progenitor cells; ESC-NPCs, ESC-derived neural progenitor cells; Heparin-MAL, heparin maleimide; hTERT, human telomerase reverse transcriptase; BMSCs, bone marrow-derived stromal/stem cells; HSPC, hematopoietic stem and progenitor cells; NA, not available

Fig. 11 Schematics highlighting the differences in the organoid formation in chemically defined and undefined hydrogel platforms



Acknowledgements TA would like to acknowledge the INSPIRE scheme, Department of Science and Technology, Government of India, for providing the fellowship. Graphical abstract was created with BioRender.com. Authors would like to acknowledge the efforts of Ms. Sampri Pal, Department of Biotechnology, Indian Institute of Technology Kharagpur, India, in proofreading the manuscript.

Author contributions TA contributed to conceptualization, writing—original draft, and writing—reviewing and editing; NC and MC performed writing—original draft; TKM contributed to conceptualization and writing—reviewing and editing; PM helped in writing—reviewing and editing.

Compliance with ethical standards

Conflict of interest All authors declare that they have no conflict of interest among themselves or with any funding agency.

Ethical approval This article does not contain any studies with human or animal subjects performed by any of the authors.

References

- Huch M, Koo B-K (2015) Modeling mouse and human development using organoid cultures. *Development* 142:3113–3125. <https://doi.org/10.1242/dev.118570>
- Kaushik G, Ponnusamy MP, Batra SK (2018) Concise review: current status of three-dimensional organoids as preclinical models. *Stem Cells* 36:1329–1340. <https://doi.org/10.1002/stem.2852>
- Kretzschmar K, Clevers H (2016) Organoids: modeling development and the stem cell niche in a dish. *Dev Cell* 38:590–600. <https://doi.org/10.1016/j.devcel.2016.08.014>
- Kim J, Koo B-K, Knoblich JA (2020) Human organoids: model systems for human biology and medicine. *Nat Rev Mol Cell Biol* 21:571–584. <https://doi.org/10.1038/s41580-020-0259-3>

5. Dedhia PH, Bertaux-Skeirik N, Zavros Y, Spence JR (2016) Organoid models of human gastrointestinal development and disease. *Gastroenterology* 150:1098–1112. <https://doi.org/10.1053/j.gastro.2015.12.042>
6. Pastuła A, Middelhoff M, Brandtner A, Tobiasch M, Höhl B, Nuber AH, Demir IE, Neupert S, Kollmann P, Mazzuoli-Weber G, Quante M (2016) Three-dimensional gastrointestinal organoid culture in combination with nerves or fibroblasts: a method to characterize the gastrointestinal stem cell niche. *Stem Cells Int* 2016:1–16. <https://doi.org/10.1155/2016/3710836>
7. Kim G-A, Spence JR, Takayama S (2017) Bioengineering for intestinal organoid cultures. *Curr Opin Biotechnol* 47:51–58. <https://doi.org/10.1016/j.copbio.2017.05.006>
8. Takahashi Y, Takebe T, Taniguchi H (2018) Methods for generating vascularized islet-like organoids via self-condensation. *Curr Protoc Stem Cell Biol* 45:e49. <https://doi.org/10.1002/cpsc.49>
9. Abdal Dayem A, Bin LS, Kim K, Lim KM, Jeon T, Cho S-G (2019) Recent advances in organoid culture for insulin production and diabetes therapy: methods and challenges. *BMB Rep* 52:295–303. <https://doi.org/10.5483/BMBRep.2019.52.5.089>
10. Hu H, Gehart H, Artegiani B, López-Iglesias C, Dekkers F, Basak O, van Es J, de Sousa Chuva, Lopes SM, Begthel H, Korving J, van den Born M, Zou C, Quirk C, Chiriboga L, Rice CM, Ma S, Rios A, Peters PJ, de Jong YP, Clevers H (2018) Long-term expansion of functional mouse and human hepatocytes as 3D organoids. *Cell* 175:1591–1606.e19. <https://doi.org/10.1016/j.cell.2018.11.013>
11. Asai A, Aihara E, Watson C, Mourya R, Mizuochi T, Shivakumar P, Phelan K, Mayhew C, Helmrath M, Takebe T, Wells J, Bezerra JA (2017) Paracrine signals regulate human liver organoid maturation from induced pluripotent stem cells. *Development* 144:1056–1064. <https://doi.org/10.1242/dev.142794>
12. Morizane R, Bonventre JV (2017) Kidney organoids: a translational journey. *Trends Mol Med* 23:246–263. <https://doi.org/10.1016/j.molmed.2017.01.001>
13. Kumar SV, Er PX, Lawlor KT, Motazedian A, Scurr M, Ghorbali I, Combes AN, Zappia L, Oshlack A, Stanley EG, Little MH (2019) Kidney micro-organoids in suspension culture as a scalable source of human pluripotent stem cell-derived kidney cells. *Development* 146:dev172361. <https://doi.org/10.1242/dev.172361>
14. Boretto M, Cox B, Noben M, Hendriks N, Fassbender A, Roose H, Amant F, Timmerman D, Tomassetti C, Vanhie A, Meuleman C, Ferrante M, Vankelecom H (2017) Development of organoids from mouse and human endometrium showing endometrial epithelium physiology and long-term expandability. *Development* 144:1775–1786. <https://doi.org/10.1242/dev.148478>
15. Fitzgerald HC, Dhakal P, Behura SK, Schust DJ, Spencer TE (2019) Self-renewing endometrial epithelial organoids of the human uterus. *Proc Natl Acad Sci* 116:23132–23142. <https://doi.org/10.1073/pnas.1915389116>
16. Nugraha B, Buono MF, Boehmer L, Hoerstrup SP, Emmert MY (2019) Human cardiac organoids for disease modeling. *Clin Pharmacol Ther* 105:79–85. <https://doi.org/10.1002/cpt.1286>
17. Hoang P, Wang J, Conklin BR, Healy KE, Ma Z (2018) Generation of spatial-patterned early-developing cardiac organoids using human pluripotent stem cells. *Nat Protoc* 13:723–737. <https://doi.org/10.1038/nprot.2018.006>
18. Llonch S, Carido M, Ader M (2018) Organoid technology for retinal repair. *Dev Biol* 433:132–143. <https://doi.org/10.1016/j.ydbio.2017.09.028>
19. Völkner M, Zschätzsch M, Rostovskaya M, Overall RW, Busskamp V, Anastassiadis K, Karl MO (2016) Retinal organoids from pluripotent stem cells efficiently recapitulate retinogenesis. *Stem Cell Reports* 6:525–538. <https://doi.org/10.1016/j.stemcr.2016.03.001>
20. Sachs N, Papaspyropoulos A, Zomer-van Ommen DD, Heo I, Böttinger L, Klay D, Weeber F, Huelsz-Prince G, Iakobachvili N, Amatngalim GD, Ligt J, Hoeck A, Proost N, Viveen MC, Lyubimova A, Teeven L, Derakhshan S, Korving J, Begthel H, Dekkers JF, Kumawat K, Ramos E, Oosterhout MF, Offerhaus GJ, Wiener DJ, Olimpio EP, Dijkstra KK, Smit EF, Linden M, Jaksani S, Ven M, Jonkers J, Rios AC, Voest EE, Moorsel CH, Ent CK, Cuppen E, Oudenaarden A, Coenjaerts FE, Meyaard L, Bont LJ, Peters PJ, Tans SJ, Zon JS, Boj SF, Vries RG, Beekman JM, Clevers H (2019) Long-term expanding human airway organoids for disease modeling. *EMBO J* 38:100300. <https://doi.org/10.15252/embj.2018100300>
21. Tan Q, Choi KM, Sicard D, Tschumperlin DJ (2017) Human airway organoid engineering as a step toward lung regeneration and disease modeling. *Biomaterials* 113:118–132. <https://doi.org/10.1016/j.biomaterials.2016.10.046>
22. Poznansky MC, Evans RH, Foxall RB, Olszak IT, Piascik AH, Hartman KE, Brander C, Meyer TH, Pykett MJ, Chabner KT, Kalams SA, Rosenzweig M, Scadden DT (2000) Efficient generation of human T cells from a tissue-engineered thymic organoid. *Nat Biotechnol* 18:729–734. <https://doi.org/10.1038/77288>
23. Bar-Ephraim YE, Kretzschmar K, Clevers H (2020) Organoids in immunological research. *Nat Rev Immunol* 20:279–293. <https://doi.org/10.1038/s41577-019-0248-y>
24. Kelava I, Lancaster MA (2016) Dishing out mini-brains: Current progress and future prospects in brain organoid research. *Dev Biol* 420:199–209. <https://doi.org/10.1016/j.ydbio.2016.06.037>
25. Heide M, Huttner WB, Mora-Bermúdez F (2018) Brain organoids as models to study human neocortex development and evolution. *Curr Opin Cell Biol* 55:8–16. <https://doi.org/10.1016/j.ceb.2018.06.006>
26. Lei M, Schumacher LJ, Lai Y-C, Juan W-T, Yeh C-Y, Wu P, Jiang T-X, Baker RE, Widelitz RB, Yang L, Chuong C-M (2017) Self-organization process in newborn skin organoid formation inspires strategy to restore hair regeneration of adult cells. *Proc Natl Acad Sci* 114:E7101–E7110. <https://doi.org/10.1073/pnas.1700475114>
27. Kim Y, Ju JH (2019) Generation of 3D skin organoid from cord blood-derived induced pluripotent stem cells. *J Vis Exp*. <https://doi.org/10.3791/59297>
28. Aisenbrey EA, Murphy WL (2020) Synthetic alternatives to Matrigel. *Nat Rev Mater* 5:539–551. <https://doi.org/10.1038/s41578-020-0199-8>
29. Blondel D, Lutolf MP (2019) Bioinspired hydrogels for 3D organoid culture. *Chim Int J Chem* 73:81–85. <https://doi.org/10.2533/chimia.2019.81>
30. Holloway EM, Capeling MM, Spence JR (2019) Biologically inspired approaches to enhance human organoid complexity. *Development* 146:dev166173. <https://doi.org/10.1242/dev.166173>
31. Jin Y, Kim J, Lee JS, Min S, Kim S, Ahn D-H, Kim Y-G, Cho S-W (2018) Vascularized liver organoids generated using induced hepatic tissue and dynamic liver-specific microenvironment as a drug testing platform. *Adv Funct Mater* 28:1801954. <https://doi.org/10.1002/adfm.201801954>
32. Hun M, Barsanti M, Wong K, Ramshaw J, Werkmeister J, Chidgey AP (2017) Native thymic extracellular matrix improves in vivo thymic organoid T cell output, and drives in vitro thymic epithelial cell differentiation. *Biomaterials* 118:1–15. <https://doi.org/10.1016/j.biomaterials.2016.11.054>
33. Mollica PA, Booth-Creech EN, Reid JA, Zamponi M, Sullivan SM, Palmer X-L, Sachs PC, Bruno RD (2019) 3D bio-printed mammary organoids and tumoroids in human mammary derived ECM hydrogels. *Acta Biomater* 95:201–213. <https://doi.org/10.1016/j.actbio.2019.06.017>

34. Bi H, Karanth SS, Ye K, Stein R, Jin S (2020) Decellularized tissue matrix enhances self-assembly of islet organoids from pluripotent stem cell differentiation. *ACS Biomater Sci Eng* 6:4155–4165. <https://doi.org/10.1021/acsbomaterials.0c00088>
35. Magno V, Meinhardt A, Werner C (2020) Polymer hydrogels to guide organotypic and organoid cultures. *Adv Funct Mater* 30:2000097. <https://doi.org/10.1002/adfm.202000097>
36. Giobbe GG, Crowley C, Luni C, Campinoti S, Khedr M, Kretzschmar K, De Santis MM, Zambaiti E, Michielin F, Meran L, Hu Q, van Son G, Urbani L, Manfredi A, Giomo M, Eaton S, Cacchiarelli D, Li VSW, Clevers H, Bonfanti P, Elvassore N, De Coppi P (2019) Extracellular matrix hydrogel derived from decellularized tissues enables endodermal organoid culture. *Nat Commun* 10:5658. <https://doi.org/10.1038/s41467-019-13605-4>
37. Agarwal T, Narayan R, Maji S, Ghosh SK, Maiti TK (2018) Decellularized caprine liver extracellular matrix as a 2D substrate coating and 3D hydrogel platform for vascularized liver tissue engineering. *J Tissue Eng Regen Med* 12:e1678–e1690. <https://doi.org/10.1002/term.2594>
38. Kaukonen R, Jacquemet G, Hamidi H, Ivaska J (2017) Cell-derived matrices for studying cell proliferation and directional migration in a complex 3D microenvironment. *Nat Protoc* 12:2376–2390. <https://doi.org/10.1038/nprot.2017.107>
39. Ventre M, Netti P (2016) Controlling cell functions and fate with surfaces and hydrogels: the role of material features in cell adhesion and signal transduction. *Gels* 2:12. <https://doi.org/10.3390/gels2010012>
40. Chen AA, Thomas DK, Ong LL, Schwartz RE, Golub TR, Bhatia SN (2011) Humanized mice with ectopic artificial liver tissues. *Proc Natl Acad Sci* 108:11842–11847. <https://doi.org/10.1073/pnas.1101791108>
41. Li J, Chen Y, Kawazoe N, Chen G (2018) Ligand density-dependent influence of arginine–glycine–aspartate functionalized gold nanoparticles on osteogenic and adipogenic differentiation of mesenchymal stem cells. *Nano Res* 11:1247–1261. <https://doi.org/10.1007/s12274-017-1738-5>
42. Meyer M (2019) Processing of collagen based biomaterials and the resulting materials properties. *Biomed Eng Online* 18:24. <https://doi.org/10.1186/s12938-019-0647-0>
43. Echave MC, Burgo LS, Pedraz JL, Orive G (2017) Gelatin as biomaterial for tissue engineering. *Curr Pharm Des* 23:3567–3584. <https://doi.org/10.2174/0929867324666170511123101>
44. Huang W, Navarro-Serer B, Jeong YJ, Chianchini P, Xia L, Luchini C, Veronese N, Dowiak C, Ng T, Trujillo MA, Huang B, Pflüger MJ, Macgregor-Das AM, Lionheart G, Jones D, Fujikura K, Nguyen-Ngoc K-V, Neumann NM, Groot VP, Hasanain A, van Oosten AF, Fischer SE, Gallinger S, Singhi AD, Zureikat AH, Brand RE, Gaida MM, Heinrich S, Burkhart RA, He J, Wolfgang CL, Goggins MG, Thompson ED, Roberts NJ, Ewald AJ, Wood LD (2020) Pattern of invasion in human pancreatic cancer organoids is associated with loss of SMAD4 and clinical outcome. *Cancer Res* 80:2804–2817. <https://doi.org/10.1158/0008-5472.CAN-19-1523>
45. Capeling M, Huang S, Mulero-Russe A, Cieza R, Tsai Y-H, Garcia A, Hill DR (2020) Generation of small intestinal organoids for experimental intestinal physiology. *Methods Cell Biol* 159:143–174. <https://doi.org/10.1016/bs.mcb.2020.03.007>
46. Sachs N, Tsukamoto Y, Kujala P, Peters PJ, Clevers H (2017) Intestinal epithelial organoids fuse to form self-organizing tubes in floating collagen gels. *Development* 144:1107–1112. <https://doi.org/10.1242/dev.143933>
47. Jabaji Z, Brinkley GJ, Khalil HA, Sears CM, Lei NY, Lewis M, Stelzner M, Martín MG, Dunn JCY (2014) Type I collagen as an extracellular matrix for the in vitro growth of human small intestinal epithelium. *PLoS ONE* 9:e107814. <https://doi.org/10.1371/journal.pone.0107814>
48. Sun W, Incitti T, Migliaresi C, Quattrone A, Casarosa S, Motta A (2016) Genipin-crosslinked gelatin–silk fibroin hydrogels for modulating the behaviour of pluripotent cells. *J Tissue Eng Regen Med* 10:876–887. <https://doi.org/10.1002/term.1868>
49. Broderick EP, O'Halloran DM, Rochev YA, Griffin M, Collihan RJ, Pandit AS (2005) Enzymatic stabilization of gelatin-based scaffolds. *J Biomed Mater Res* 72B:37–42. <https://doi.org/10.1002/jbm.b.30119>
50. Zhang YS, Pi Q, van Genderen AM (2017) Microfluidic bioprinting for engineering vascularized tissues and organoids. *J Vis Exp*. <https://doi.org/10.3791/55957>
51. Ahmed TAE, Dare EV, Hincke M (2008) Fibrin: a versatile scaffold for tissue engineering applications. *Tissue Eng Part B Rev* 14:199–215. <https://doi.org/10.1089/ten.teb.2007.0435>
52. Broguiere N, Isenmann L, Hirt C, Ringel T, Placzek S, Cavalli E, Ringnald F, Villiger L, Züllig R, Lehmann R, Rogler G, Heim MH, Schüler J, Zenobi-Wong M, Schwank G (2018) Growth of epithelial organoids in a defined hydrogel. *Adv Mater* 30:1801621. <https://doi.org/10.1002/adma.201801621>
53. Wang Y, Liu H, Zhang M, Wang H, Chen W, Qin J (2020) One-step synthesis of composite hydrogel capsules to support liver organoid generation from hiPSCs. *Biomater Sci* 8:5476–5488. <https://doi.org/10.1039/D0BM01085E>
54. Collins MN, Birkinshaw C (2013) Hyaluronic acid based scaffolds for tissue engineering—a review. *Carbohydr Polym* 92:1262–1279. <https://doi.org/10.1016/j.carbpol.2012.10.028>
55. Khunmanee S, Jeong Y, Park H (2017) Crosslinking method of hyaluronic-based hydrogel for biomedical applications. *J Tissue Eng* 8:204173141772646. <https://doi.org/10.1177/2041731417726464>
56. Georgakopoulos N, Prior N, Angres B, Mastrogiovanni G, Cagan A, Harrison D, Hindley CJ, Arnes-Benito R, Liau S-S, Curd A, Ivory N, Simons BD, Martincorena I, Wurst H, Saeb-Parsy K, Huch M (2020) Long-term expansion, genomic stability and in vivo safety of adult human pancreas organoids. *BMC Dev Biol* 20:4. <https://doi.org/10.1186/s12861-020-0209-5>
57. Liang Y, Kiick KL (2014) Heparin-functionalized polymeric biomaterials in tissue engineering and drug delivery applications. *Acta Biomater* 10:1588–1600. <https://doi.org/10.1016/j.actbio.2013.07.031>
58. Schirmer L, Chwalek K, Tsurkan MV, Freudenberg U, Werner C (2020) Glycosaminoglycan-based hydrogels with programmable host reactions. *Biomaterials* 228:119557. <https://doi.org/10.1016/j.biomaterials.2019.119557>
59. Weber HM, Tsurkan MV, Magno V, Freudenberg U, Werner C (2017) Heparin-based hydrogels induce human renal tubulogenesis in vitro. *Acta Biomater* 57:59–69. <https://doi.org/10.1016/j.actbio.2017.05.035>
60. Nowak M, Freudenberg U, Tsurkan MV, Werner C, Levental KR (2017) Modular GAG-matrices to promote mammary epithelial morphogenesis in vitro. *Biomaterials* 112:20–30. <https://doi.org/10.1016/j.biomaterials.2016.10.007>
61. Sun J, Tan H (2013) Alginate-based biomaterials for regenerative medicine applications. *Materials (Basel)* 6:1285–1309. <https://doi.org/10.3390/ma6041285>
62. Agarwal T, Kabiraj P, Narayana GH, Kulanthaivel S, Kasiviswanathan U, Pal K, Giri S, Maiti TK, Banerjee I (2016) Alginate bead based hexagonal close packed 3D implant for bone tissue engineering. *ACS Appl Mater Interfaces* 8:32132–32145. <https://doi.org/10.1021/acsami.6b08512>
63. Kulanthaivel S, Rathnam VSS, Agarwal T, Pradhan S, Pal K, Giri S, Maiti TK, Banerjee I (2017) Gum tragacanth–alginate beads as proangiogenic–osteogenic cell encapsulation systems for bone tissue engineering. *J Mater Chem B* 5:4177–4189. <https://doi.org/10.1039/C7TB00390K>

64. Capeling MM, Czerwinski M, Huang S, Tsai Y-H, Wu A, Nagy MS, Juliar B, Sundaram N, Song Y, Han WM, Takayama S, Alsborg E, Garcia AJ, Helmrath M, Putnam AJ, Spence JR (2019) Nonadhesive alginate hydrogels support growth of pluripotent stem cell-derived intestinal organoids. *Stem Cell Reports* 12:381–394. <https://doi.org/10.1016/j.stemcr.2018.12.001>
65. Agarwal T, Narayan R, Maji S, Behera S, Kulanthaivel S, Maiti TK, Banerjee I, Pal K, Giri S (2016) Gelatin/carboxymethyl chitosan based scaffolds for dermal tissue engineering applications. *Int J Biol Macromol* 93:1499–1506. <https://doi.org/10.1016/j.ijbiomac.2016.04.028>
66. Croisier F, Jérôme C (2013) Chitosan-based biomaterials for tissue engineering. *Eur Polym J* 49:780–792. <https://doi.org/10.1016/j.eurpolymj.2012.12.009>
67. Lindborg BA, Brekke JH, Vegoe AL, Ulrich CB, Haider KT, Subramaniam S, Venhuizen SL, Eide CR, Orchard PJ, Chen W, Wang Q, Pelaez F, Scott CM, Kakkoli E, Keirstead SA, Dutton JR, Tolar J, O'Brien TD (2016) Rapid induction of cerebral organoids from human induced pluripotent stem cells using a chemically defined hydrogel and defined cell culture medium. *Stem Cells Transl Med* 5:970–979. <https://doi.org/10.5966/sctm.2015-0305>
68. Argüelles-Monal W, Lizardi-Mendoza J, Fernández-Quiroz D, Recillas-Mota M, Montiel-Herrera M (2018) Chitosan derivatives: introducing new functionalities with a controlled molecular architecture for innovative materials. *Polymers (Basel)* 10:342. <https://doi.org/10.3390/polym10030342>
69. Zhang Y, Tang C, Span PN, Rowan AE, Aalders TW, Schalken JA, Adema GJ, Kouwer PHJ, Zegers MMP, Ansems M (2020) Polyisocyanide hydrogels as a tunable platform for mammary gland organoid formation. *Adv Sci* 7:2001797. <https://doi.org/10.1002/adv.202001797>
70. Unal AZ, West JL (2020) Synthetic ECM: Bioactive synthetic hydrogels for 3D tissue engineering. *Bioconj Chem* 31:2253–2271. <https://doi.org/10.1021/acs.bioconjchem.0c00270>
71. D'souza AA, Shegokar R, (2016) Polyethylene glycol (PEG): a versatile polymer for pharmaceutical applications. *Expert Opin Drug Deliv* 13:1257–1275. <https://doi.org/10.1080/17425247.2016.1182485>
72. Chen G, Tang W, Wang X, Zhao X, Chen C, Zhu Z (2019) Applications of hydrogels with special physical properties in biomedicine. *Polymers (Basel)* 11:1420. <https://doi.org/10.3390/polym11091420>
73. Cruz-Acuña R, Quirós M, Farkas AE, Dedhia PH, Huang S, Siuda D, García-Hernández V, Miller AJ, Spence JR, Nusrat A, García AJ (2017) Synthetic hydrogels for human intestinal organoid generation and colonic wound repair. *Nat Cell Biol* 19:1326–1335. <https://doi.org/10.1038/ncb3632>
74. Hernandez-Gordillo V, Kassis T, Lampejo A, Choi G, Gamboa ME, Gnecco JS, Brown A, Breault DT, Carrier R, Griffith LG (2020) Fully synthetic matrices for in vitro culture of primary human intestinal enteroids and endometrial organoids. *Biomaterials* 254:120125. <https://doi.org/10.1016/j.biomaterials.2020.120125>
75. Ye S, Boeter JWB, Mihajlovic M, Steenbeek FG, Wolferen ME, Oosterhoff LA, Marsee A, Caiazzo M, Laan LJW, Penning LC, Vermonden T, Spee B, Schneeberger K (2020) A chemically defined hydrogel for human liver organoid culture. *Adv Funct Mater* 30:2000893. <https://doi.org/10.1002/adfm.202000893>
76. Zimoch J, Padial JS, Klar AS, Vallmajo-Martin Q, Meuli M, Biedermann T, Wilson CJ, Rowan A, Reichmann E (2018) Polyisocyanopeptide hydrogels: A novel thermo-responsive hydrogel supporting pre-vascularization and the development of organotypic structures. *Acta Biomater* 70:129–139. <https://doi.org/10.1016/j.actbio.2018.01.042>
77. Gu L, Shan T, Ma Y, Tay FR, Niu L (2019) Novel biomedical applications of crosslinked collagen. *Trends Biotechnol* 37:464–491. <https://doi.org/10.1016/j.tibtech.2018.10.007>
78. Soroushanova A, Delgado LM, Wu Z, Shologu N, Kshirsagar A, Raghunath R, Mullen AM, Bayon Y, Pandit A, Raghunath M, Zeugolis DI (2019) The collagen suprafamily: from biosynthesis to advanced biomaterial development. *Adv Mater* 31:1801651. <https://doi.org/10.1002/adma.201801651>
79. Van Hoorick J, Tytgat L, Dobos A, Ottevaere H, Van Erps J, Thienpont H, Ovsianikov A, Dubruel P, Van Vlierberghe S (2019) (Photo-)crosslinkable gelatin derivatives for biofabrication applications. *Acta Biomater* 97:46–73. <https://doi.org/10.1016/j.actbio.2019.07.035>
80. Wang X, Ao Q, Tian X, Fan J, Tong H, Hou W, Bai S (2017) Gelatin-based hydrogels for organ 3D bioprinting. *Polymers (Basel)* 9:401. <https://doi.org/10.3390/polym9090401>
81. de Melo BAG, Jodat YA, Cruz EM, Benincasa JC, Shin SR, Porcionatto MA (2020) Strategies to use fibrinogen as bioink for 3D bioprinting fibrin-based soft and hard tissues. *Acta Biomater* 117:60–76. <https://doi.org/10.1016/j.actbio.2020.09.024>
82. Sakiyama-Elbert SE (2014) Incorporation of heparin into biomaterials. *Acta Biomater* 10:1581–1587. <https://doi.org/10.1016/j.actbio.2013.08.045>
83. Salwowska NM, Bebenek KA, Żądło DA, Wcisło-Dziadecka DL (2016) Physicochemical properties and application of hyaluronic acid: a systematic review. *J Cosmet Dermatol* 15:520–526. <https://doi.org/10.1111/jocd.12237>
84. Pereira H, Sousa DA, Cunha A, Andrade R, Espregueira-Mendes J, Oliveira JM, Reis RL (2018) Hyaluronic acid. In: *Osteochondral tissue engineering. Advances in experimental medicine and biology*, vol 1059. pp 137–153. https://doi.org/10.1007/978-3-319-76735-2_6
85. Rastogi P, Kandasubramanian B (2019) Review of alginate-based hydrogel bioprinting for application in tissue engineering. *Biofabrication* 11:042001. <https://doi.org/10.1088/1758-5090/ab331e>
86. Vanacker J, Amorim CA (2017) Alginate: a versatile biomaterial to encapsulate isolated ovarian follicles. *Ann Biomed Eng* 45:1633–1649. <https://doi.org/10.1007/s10439-017-1816-6>
87. Lee KY, Mooney DJ (2012) Alginate: Properties and biomedical applications. *Prog Polym Sci* 37:106–126. <https://doi.org/10.1016/j.progpolymsci.2011.06.003>
88. Muxika A, Etxabide A, Urange J, Guerrero P, de la Caba K (2017) Chitosan as a bioactive polymer: processing, properties and applications. *Int J Biol Macromol* 105:1358–1368. <https://doi.org/10.1016/j.ijbiomac.2017.07.087>
89. Muanprasat C, Chatsudthipong V (2017) Chitosan oligosaccharide: biological activities and potential therapeutic applications. *Pharmacol Ther* 170:80–97. <https://doi.org/10.1016/j.pharmthera.2016.10.013>
90. Cruz-Acuña R, Quirós M, Huang S, Siuda D, Spence JR, Nusrat A, García AJ (2018) PEG-4MAL hydrogels for human organoid generation, culture, and in vivo delivery. *Nat Protoc* 13:2102–2119. <https://doi.org/10.1038/s41596-018-0036-3>
91. Gjorevski N, Lutolf MP (2017) Synthesis and characterization of well-defined hydrogel matrices and their application to intestinal stem cell and organoid culture. *Nat Protoc* 12:2263–2274. <https://doi.org/10.1038/nprot.2017.095>
92. Vallmajo-Martin Q, Broguiere N, Millan C, Zenobi-Wong M, Ehrbar M (2020) PEG/HA hybrid hydrogels for biologically and mechanically tailorable bone marrow organoids. *Adv Funct Mater* 30:1910282. <https://doi.org/10.1002/adfm.201910282>
93. Wechsler ME, Shevchuk M, Peppas NA (2020) Developing a multidisciplinary approach for engineering stem cell organoids. *Ann Biomed Eng* 48:1895–1904. <https://doi.org/10.1007/s10439-019-02391-1>

94. Ranga A, Girgin M, Meinhardt A, Eberle D, Caiazzo M, Tanaka EM, Lutolf MP (2016) Neural tube morphogenesis in synthetic 3D microenvironments. *Proc Natl Acad Sci* 113:E6831–E6839. <https://doi.org/10.1073/pnas.1603529113>
95. Balion Z, C epla V, Svirskiene N, Svirskis G, Druceikaitė K, Inokaitis H, Rusteikaitė J, Masilionis I, Stankevičienė G, Jelin-skas T, Ul cinas A, Samanta A, Valiokas R, Jekabsone A (2020) Cerebellar cells self-assemble into functional organoids on synthetic, chemically crosslinked ECM-mimicking peptide hydrogels. *Biomolecules* 10:754. <https://doi.org/10.3390/biom10050754>
96. Agarwal T, Subramanian B, Maiti TK (2019) Liver tissue engineering: challenges and opportunities. *ACS Biomater Sci Eng* 5:4167–4182. <https://doi.org/10.1021/acsbomaterials.9b00745>
97. Miyaoka Y, Ebato K, Kato H, Arakawa S, Shimizu S, Miyajima A (2012) Hypertrophy and unconventional cell division of hepatocytes underlie liver regeneration. *Curr Biol* 22:1166–1175. <https://doi.org/10.1016/j.cub.2012.05.016>
98. Xu H, Jiao Y, Qin S, Zhao W, Chu Q, Wu K (2018) Organoid technology in disease modelling, drug development, personalized treatment and regeneration medicine. *Exp Hematol Oncol* 7:30. <https://doi.org/10.1186/s40164-018-0122-9>
99. Underhill GH, Khetani SR (2018) Bioengineered liver models for drug testing and cell differentiation studies. *Cell Mol Gastroenterol Hepatol* 5:426–439.e1. <https://doi.org/10.1016/j.jcmgh.2017.11.012>
100. Akbari S, Arslan N, Senturk S, Erdal E (2019) Next-generation liver medicine using organoid models. *Front Cell Dev Biol* 7:345. <https://doi.org/10.3389/fcell.2019.00345>
101. Sorrentino G, Rezakhani S, Yildiz E, Nuciforo S, Heim MH, Lutolf MP, Schoonjans K (2020) Mechano-modulatory synthetic niches for liver organoid derivation. *Nat Commun* 11:3416. <https://doi.org/10.1038/s41467-020-17161-0>
102. Kr uger M, Oosterhoff LA, van Wolferen ME, Schiele SA, Walther A, Geijssen N, De Laporte L, van der Laan LJW, Kock LM, Spee B (2020) Cellulose nanofibril hydrogel promotes hepatic differentiation of human liver organoids. *Adv Health Mater* 9:1901658. <https://doi.org/10.1002/adhm.201901658>
103. Hohwieler M, M uller M, Frappart P-O, Heller S (2019) Pancreatic progenitors and organoids as a prerequisite to model pancreatic diseases and cancer. *Stem Cells Int* 2019:1–11. <https://doi.org/10.1155/2019/9301382>
104. Greggio C, De Franceschi F, Figueiredo-Larsen M, Gobaa S, Ranga A, Semb H, Lutolf M, Grapin-Botton A (2013) Artificial three-dimensional niches deconstruct pancreas development in vitro. *Development* 140:4452–4462. <https://doi.org/10.1242/dev.096628>
105. Candiello J, Grandhi TSP, Goh SK, Vaidya V, Lemmon-Kishi M, Eliato KR, Ros R, Kumta PN, Rege K, Banerjee I (2018) 3D heterogeneous islet organoid generation from human embryonic stem cells using a novel engineered hydrogel platform. *Biomaterials* 177:27–39. <https://doi.org/10.1016/j.biomaterials.2018.05.031>
106. Ding B, Sun G, Liu S, Peng E, Wan M, Chen L, Jackson J, Atala A (2020) Three-dimensional renal organoids from whole kidney cells: generation, optimization, and potential application in nephrotoxicology in vitro. *Cell Transplant* 29:0963689719897066. <https://doi.org/10.1177/0963689719897066>
107. Webster AC, Nagler EV, Morton RL, Masson P (2017) Chronic kidney disease. *Lancet* 389:1238–1252. [https://doi.org/10.1016/S0140-6736\(16\)32064-5](https://doi.org/10.1016/S0140-6736(16)32064-5)
108. Garreta E, Montserrat N, Belmonte JCI (2018) Kidney organoids for disease modeling. *Oncotarget* 9:12552–12553. <https://doi.org/10.18632/oncotarget.24438>
109. Enemchukwu NO, Cruz-Acu na R, Bongiorno T, Johnson CT, Garc a JR, Sulchek T, Garc a AJ (2016) Synthetic matrices reveal contributions of ECM biophysical and biochemical properties to epithelial morphogenesis. *J Cell Biol* 212:113–124. <https://doi.org/10.1083/jcb.201506055>
110. Cruz-Acu na R, Mulero-Russe A, Clark AY, Zent R, Garc a AJ (2019) Identification of matrix physicochemical properties required for renal epithelial cell tubulogenesis by using synthetic hydrogels. *J Cell Sci* 132:jcs226639. <https://doi.org/10.1242/jcs.226639>
111. Costa J, Ahluwalia A (2019) Advances and current challenges in intestinal in vitro model engineering: a digest. *Front Bioeng Biotechnol* 7:144. <https://doi.org/10.3389/fbioe.2019.00144>
112. Qi D, Shi W, Black AR, Kuss MA, Pang X, He Y, Liu B, Duan B (2020) Repair and regeneration of small intestine: a review of current engineering approaches. *Biomaterials* 240:119832. <https://doi.org/10.1016/j.biomaterials.2020.119832>
113. Sato T, Stange DE, Ferrante M, Vries RGJ, van Es JH, van den Brink S, van Houdt WJ, Pronk A, van Gorp J, Siersema PD, Clevers H (2011) Long-term expansion of epithelial organoids from human colon, adenoma, adenocarcinoma, and Barrett's epithelium. *Gastroenterology* 141:1762–1772. <https://doi.org/10.1053/j.gastro.2011.07.050>
114. DiMarco RL, Dewi RE, Bernal G, Kuo C, Heilshorn SC (2015) Protein-engineered scaffolds for in vitro 3D culture of primary adult intestinal organoids. *Biomater Sci* 3:1376–1385. <https://doi.org/10.1039/C5BM00108K>
115. Gjorevski N, Sachs N, Manfrin A, Giger S, Bragina ME, Ord o nez-Mor an P, Clevers H, Lutolf MP (2016) Designer matrices for intestinal stem cell and organoid culture. *Nature* 539:560–564. <https://doi.org/10.1038/nature20168>
116. Florian S, Iwamoto Y, Coughlin M, Weissleder R, Mitchison TJ (2019) A human organoid system that self-organizes to recapitulate growth and differentiation of a benign mammary tumor. *Proc Natl Acad Sci* 116:11444–11453. <https://doi.org/10.1073/pnas.1702372116>
117. Gu Z-Y, Jia S-Z, Liu S, Leng J-H (2020) Endometrial organoids: a new model for the research of endometrial-related diseases. *Biol Reprod* 103:918–926. <https://doi.org/10.1093/biolre/iaaa124>
118. Graney PL, Lai K, Post S, Brito I, Cyster J, Singh A (2020) Organoid polymer functionality and mode of Klebsiella pneumoniae membrane antigen presentation regulates ex vivo germinal center epigenetics in young and aged B cells. *Adv Funct Mater* 30:2001232. <https://doi.org/10.1002/adfm.202001232>
119. Jansen LE, McCarthy TP, Lee MJ, Peyton SR (2018) A synthetic, three-dimensional bone marrow hydrogel. *bioRxiv* 275842. <https://doi.org/10.1101/275842>
120. Bejoy J, Wang Z, Bijonowski B, Yang M, Ma T, Sang Q-X, Li Y (2018) Differential effects of heparin and hyaluronic acid on neural patterning of human induced pluripotent stem cells. *ACS Biomater Sci Eng* 4:4354–4366. <https://doi.org/10.1021/acsbomaterials.8b01142>
121. Ng S, Tan WJ, Pek MMX, Tan M-H, Kurisawa M (2019) Mechanically and chemically defined hydrogel matrices for patient-derived colorectal tumor organoid culture. *Biomaterials* 219:119400. <https://doi.org/10.1016/j.biomaterials.2019.119400>
122. DiMarco RL, Su J, Yan KS, Dewi R, Kuo CJ, Heilshorn SC (2014) Engineering of three-dimensional microenvironments to promote contractile behavior in primary intestinal organoids. *Integr Biol* 6:127–142. <https://doi.org/10.1039/C3IB40188J>
123. Barry C, Schmitz MT, Propson NE, Hou Z, Zhang J, Nguyen BK, Bolin JM, Jiang P, McIntosh BE, Probasco MD, Swanson S, Stewart R, Thomson JA, Schwartz MP, Murphy WL (2017) Uniform neural tissue models produced on synthetic hydrogels using standard culture techniques. *Exp Biol Med* 242:1679–1689. <https://doi.org/10.1177/1535370217715028>

124. Meinhardt A, Eberle D, Tazaki A, Ranga A, Niesche M, Wilsch-Bräuninger M, Stec A, Schackert G, Lutolf M, Tanaka EM (2014) 3D Reconstitution of the patterned neural tube from embryonic stem cells. *Stem Cell Reports* 3:987–999. <https://doi.org/10.1016/j.stemcr.2014.09.020>
125. Yavitt FM, Brown TE, Hushka EA, Brown ME, Gjorevski N, Dempsey PJ, Lutolf MP, Anseth KS (2020) The effect of thiol structure on allyl sulfide photodegradable hydrogels and their application as a degradable scaffold for organoid passaging. *Adv Mater* 32:1905366. <https://doi.org/10.1002/adma.201905366>
126. Bergenheim F, Fregni G, Buchanan CF, Riis LB, Heulot M, Touati J, Seidelin JB, Rizzi SC, Nielsen OH (2020) A fully defined 3D matrix for ex vivo expansion of human colonic organoids from biopsy tissue. *Biomaterials* 262:120248. <https://doi.org/10.1016/j.biomaterials.2020.120248>
127. Klotz BJ, Oosterhoff LA, Utomo L, Lim KS, Vallmajo-Martin Q, Clevers H, Woodfield TBF, Rosenberg AJWP, Malda J, Ehrbar M, Spee B, Gawlitta D (2019) A versatile biosynthetic hydrogel platform for engineering of tissue analogues. *Adv Healthc Mater* 8:1900979. <https://doi.org/10.1002/adhm.201900979>
128. Astashkina AI, Mann BK, Prestwich GD, Grainger DW (2012) A 3-D organoid kidney culture model engineered for high-throughput nephrotoxicity assays. *Biomaterials* 33:4700–4711. <https://doi.org/10.1016/j.biomaterials.2012.02.063>
129. Tian YF, Ahn H, Schneider RS, Yang SN, Roman-Gonzalez L, Melnick AM, Cerchietti L, Singh A (2015) Integrin-specific hydrogels as adaptable tumor organoids for malignant B and T cells. *Biomaterials* 73:110–119. <https://doi.org/10.1016/j.biomaterials.2015.09.007>
130. Kaylan KB, Ermilova V, Yada RC, Underhill GH (2016) Combinatorial microenvironmental regulation of liver progenitor differentiation by Notch ligands. *TGF β and extracellular matrix Sci Rep* 6:23490. <https://doi.org/10.1038/srep23490>
131. Kourouklis AP, Kaylan KB, Underhill GH (2016) Substrate stiffness and matrix composition coordinately control the differentiation of liver progenitor cells. *Biomaterials* 99:82–94. <https://doi.org/10.1016/j.biomaterials.2016.05.016>
132. Kloxin AM, Kasko AM, Salinas CN, Anseth KS (2009) Photodegradable hydrogels for dynamic tuning of physical and chemical properties. *Science* (80-) 324:59–63. <https://doi.org/10.1126/science.1169494>
133. Rosales AM, Anseth KS (2016) The design of reversible hydrogels to capture extracellular matrix dynamics. *Nat Rev Mater* 1:15012. <https://doi.org/10.1038/natrevmats.2015.12>
134. Mohamed MA, Fallahi A, El-Sokkary AMA, Salehi S, Akl MA, Jafari A, Tamayol A, Fenniri H, Khademhosseini A, Andreadis ST, Cheng C (2019) Stimuli-responsive hydrogels for manipulation of cell microenvironment: from chemistry to biofabrication technology. *Prog Polym Sci* 98:101147. <https://doi.org/10.1016/j.progpolymsci.2019.101147>
135. Li X, Su X (2018) Multifunctional smart hydrogels: potential in tissue engineering and cancer therapy. *J Mater Chem B* 6:4714–4730. <https://doi.org/10.1039/C8TB01078A>